Calcium Oscillations

R Thul[1], T C Bellamy[2], H L Roderick[2,3], M D Bootman[2], and S Coombes[1]

[1] School of Mathematical Sciences, University of Nottingham, Nottingham, NG7 2RD, UK.
[2] Laboratory of Molecular Signalling, The Babraham Institute, Babraham, Cambridge, CB22 3AT, UK.
[3] Department of Pharmacology, University of Cambridge, Tennis Court Road, Cambridge, CB2 1PD, UK.

Summary. Changes in cellular Ca^{2+} concentration control a wide range of physiological processes, from the subsecond release of synaptic neurotransmitters, to the regulation of gene expression over months or years. Ca^{2+} can also trigger cell death through both apoptosis and necrosis, and so the regulation of cellular Ca^{2+} concentration must be tightly controlled through the concerted action of pumps, channels and buffers that transport Ca^{2+} into and out of the cell cytoplasm. A hallmark of cellular Ca^{2+} signalling is its spatiotemporal complexity: stimulation of cells by a hormone or neurotransmitter leads to oscillations in cytoplasmic Ca^{2+} concentration that can vary markedly in time course, amplitude, frequency, and spatial range.

In this chapter we review some of the biological roles of Ca^{2+}, the experimental characterisation of complex dynamic changes in Ca^{2+} concentration, and attempts to explain this complexity using computational models. We consider the "toolkit" of cellular proteins which influence Ca^{2+} concentration, describe mechanistic models of key elements of the toolkit, and fit these into the framework of whole cell models of Ca^{2+} oscillations and waves. Finally, we will touch on recent efforts to use stochastic modelling to elucidate elementary Ca^{2+} signal events, and how these may evolve into global signals.

Key words: Calcium, IP_3 receptor, ryanodine receptor, mitochondria, SERCA pumps, De Young–Keizer model, Li–Rinzel model, Tang–Othmer model, excitable system, Hopf bifurcation, threshold model, fire-diffuse-fire model, stochastic modelling

1 Introduction

Biological cells use calcium (Ca^{2+}) to control many of their activities [11]. Cells draw on both intracellular and extracellular Ca^{2+} sources to generate signals that transduce exogenous stimulation into physiological output [21]. It is well known that prolonged elevations of Ca^{2+} lead to cell damage or death, so cells generally limit the temporal and spatial extent of their intracellular Ca^{2+} rises. Over the past thirty years, Ca^{2+} oscillations have emerged as a ubiquitous paradigm for cellular signal transduction [8, 5, 145]. It is generally believed that by utilising brief pulses of Ca^{2+}, instead of tonic rises, cells avoid the deleterious effects of sustained cytosolic Ca^{2+} levels. Furthermore, cells also benefit from the greater fidelity inherent in frequency-modulated, as compared to amplitude-modulated, signalling [6]. A simple Medline search for 'calcium oscillations' highlights over 3260 articles since 1980.

Ca^{2+} oscillations are now routinely recorded using fluorescent probes, but were previously characterised using techniques such as bioluminescence and measurement of membrane potential fluctuations [154, 157]. Indeed, it was the latter technique that provided some of the first indications that Ca^{2+} oscillations could provide specificity and longevity in cellular signalling, whereas sustained Ca^{2+} signals caused desensitisation [127]. The influx of Ca^{2+} from the extracellular space [120, 63] and release of Ca^{2+} from intracellular stores can both give rise to pulsatile cytosolic Ca^{2+} signals.

Ca^{2+} oscillations are initiated at the moment of fertilisation in vertebrates [30, 58, 98], and continue through life to regulate numerous physiological processes including cell maturation and differentiation [25], cell cycle progression [72], mitochondrial respiration [57], chemotaxis [92], secretion [93] and gene transcription [35]. They occur in vertebrates [5], plants [94, 140] and invertebrates [39]. Ca^{2+} oscillations have been recorded from a vast number of different cell types. It is evident that the pattern of Ca^{2+} oscillation varies substantially between cell types [7], and even between cells of the same type [110], due to the expression of cell-specific Ca^{2+} signalling proteomes [11]. Thus, cells can express different combinations and concentrations of the various Ca^{2+} pumps, buffers and channels that comprise a "toolkit" of Ca^{2+} regulatory proteins. Ca^{2+} oscillation patterns can be roughly segregated into Ca^{2+} transients with a random occurrence, those having a sinusoidal appearance [52] and periodic Ca^{2+} oscillations arising from a steady baseline cytosolic Ca^{2+} concentration [115, 20]. Of these different types, the baseline Ca^{2+} oscillations have been the most widely studied, and are largely the focus of this chapter.

Baseline Ca^{2+} oscillations are thought to arise due to periodic release of Ca^{2+} from intracellular stores via intracellular Ca^{2+} channels. Although a number of novel Ca^{2+}-releasing messengers and pathways have been identified recently [21], the generation of baseline Ca^{2+} oscillations is generally considered to be due activation of two types of intracellular Ca^{2+} channel; inositol 1,4,5-trisphosphate (IP_3) receptors and ryanodine receptors. IP_3 receptors (IP_3Rs) are large ($\sim$ 1200 kDa) tetrameric proteins, with an amino-terminal domain projecting into the cytoplasm, and an integral Ca^{2+} channel formed by six membrane-spanning regions in the carboxy-terminal portion of each subunit [144]. IP_3 binding within residues 226-576 of the amino terminus causes a conformational change that promotes channel opening [23]. Between the IP_3 binding site and the transmembrane regions is a large stretch of amino acids where a significant proportion of regulatory interactions occur. IP_3Rs are expressed and participate in Ca^{2+} release within almost all mammalian tissue, although their function in some cell types is unclear. Three IP_3R isoforms have been cloned and splice variants have been described, leading to the possibility of heteromultimeric channels with distinctive properties based on their subunit content. Although IP_3 is necessary for channel opening, the activation of IP_3Rs is complex and their open probability is dependent on the ambient Ca^{2+} concentration. Up to approximately 500 nM, Ca^{2+} works synergistically with IP_3 to activate IP_3Rs . At higher concentrations, cytosolic Ca^{2+} inhibits IP_3R opening [45, 13, 65, 66].

Ryanodine receptors are structurally and functionally homologous to IP_3 receptors, albeit that they have approximately twice their mass [10]. There are three cloned forms of the ryanodine receptor. Similar to IP_3Rs, ryanodine receptor opening displays a 'bell-shaped' dependence on cytosolic Ca^{2+} concentration, although they are generally activated and inhibited by slightly higher Ca^{2+} levels [13]. Both IP_3Rs and ryanodine receptors can therefore operate as Ca^{2+} -activated Ca^{2+} release (CICR) channels; a property that is believed to lead to the autocatalytic release of Ca^{2+} during the upstroke of a Ca^{2+} oscillation [114, 130, 97]. The inhibition of IP_3R and ryanodine receptor opening by high levels of cytosolic Ca^{2+} provides a negative

feedback mechanism that will terminate Ca^{2+} release, and prevent deleterious Ca^{2+} elevations [38]. It is possible that IP_3Rs may also undergo a long-term desensitisation process that can also cause Ca^{2+} release to cease [56].

IP_3Rs are almost ubiquitously expressed within mammals, whereas ryanodine receptors have a more limited tissue distribution [4, 134]. Furthermore, whilst there appears to be considerable functional redundancy between the three IP_3R isoforms, the different types of ryanodine receptor have distinct expression patterns and gating mechanisms. Type 2 ryanodine receptors, for example, are substantially expressed in the heart, where they operate as CICR channels to generate the Ca^{2+} signal that triggers cardiac contraction during each heartbeat [22]. In contrast, type 1 ryanodine receptors are largely expressed in skeletal muscle. They also provide the Ca^{2+} signal necessary to trigger muscle contraction. However, although isolated type 1 ryanodine receptors can work as CICR channels, within the intact muscle they are actually activated through direct protein-protein interactions [133].

The effect of Ca^{2+} on IP_3Rs and ryanodine receptors illustrates the complex regulation of these channel. However, although their modulation by Ca^{2+} is important, significant control of these channels is manifest by covalent modification and numerous allosteric interactions. In particular, their interaction with accessory proteins is uncovering new regulatory mechanisms and shedding light on novel aspects of biology in which these Ca^{2+} channels are involved [113, 59]. It is emerging that IP_3Rs and ryanodine receptors simultaneously bind a multitude of accessory proteins that impact their cellular location and functionality. Some of these proteins, e.g. Bcl-2, are regulators of critical cellular events. Others are enzymes, e.g. protein kinase A, which regulate the phosphorylation status of the channels and also convey information distinct from increases in Ca^{2+}. It therefore appears that IP_3Rs and ryanodine receptors are focal points for the convergence of multiple signal transduction pathways. They can modulate cellular activities through Ca^{2+} release, but in addition they may act as a signalling nexus to bring proteins into close proximity. Both IP_3Rs and ryanodine receptors have been shown to underlie Ca^{2+} oscillations in various cell types. In some cells, either IP_3Rs or ryanodine receptors are active [104], although there are numerous examples of both channel types working synergistically to generate Ca^{2+} oscillations [15].

Baseline Ca^{2+} oscillations typically have a rapid upstroke from the resting Ca^{2+} concentration, and the peak cytosolic Ca^{2+} signal is generally attained within a few seconds [9]. The recovery of the Ca^{2+} signal is generally slower, and requires the Ca^{2+} to be pumped either into mitochondria, out of the cell or re-sequestered into the intracellular stores. The spatial correlate of a Ca^{2+} oscillation is a Ca^{2+} wave (or 'tide') [19]. Due to the autocatalytic activity of IP_3Rs and ryanodine receptors, subcellular Ca^{2+} events can trigger propagating Ca^{2+} signals that can passage throughout a cell [116]. The extent of Ca^{2+} wave propagation depends on the degree of cellular stimulation [19, 106], i.e. the degree of excitability of the intracellular Ca^{2+} release channels. Ca^{2+} waves can also diffuse through gap junctions to initiate Ca^{2+} signals in neighbouring cells [16]. In this way, confluent cells layers can display synchronised Ca^{2+} signals [112, 67, 118, 102].

A noteable characteristic of Ca^{2+} oscillations is that even within a single cell their amplitude and kinetic parameters can depend on the nature of the stimulus and its concentration [115]. For example, pancreatic acinar cells secrete digestive enzymes into the small intestine in response to cholecystokinin or acetylcholine. The secretion of enzyme-containing zymogen granules is triggered by the Ca^{2+} oscillations that occur when cholecystokinin or acetylcholine are applied. Within the same pancreatic acinar cell, cholecystokinin and acetylcholine generate Ca^{2+} oscillations with an

initial sharp rising phase. However, when stimulated with cholecystokinin, the Ca^{2+} oscillations tend to show a secondary, longer-lasting, component [109].

One of the most widely studied features of Ca^{2+} oscillations is the dependence of their frequency on the strength of external stimulation [115, 55]. This concept generally applies to baseline Ca^{2+} spiking. Since, in cells that display either sinusoidal Ca^{2+} oscillations or random Ca^{2+} fluctuations the frequency of the Ca^{2+} elevations can be insensitive to stimulus strength [52]. Sinusoidal Ca^{2+} oscillations have been suggested to occur due to negative feedback regulation of either IP_3 production or IP_3R activity [14]. By controlling oscillation frequency, cells can precisely regulate their Ca^{2+}-dependent activities in a way that is graded with the level of stimulus. Cells possess a substantial number of proteins that can bind Ca^{2+}, either directly or through an intermediary such as calmodulin, and are either activated or inhibited when Ca^{2+} is bound. By 'counting' individual Ca^{2+} oscillations over time, cellular processes can be switched on or off [33]. A well-known example of an enzyme that has the ability to decode the frequency of Ca^{2+} spikes and subsequently modulate a variety of cellular activities is Ca^{2+}/calmodulin-dependent kinase [121].

2 Modelling Ca^{2+} dynamics

The striking spatiotemporal complexity of cytoplasmic Ca^{2+} signals, as outlined in the previous section, arises from the interplay of numerous cellular sources and sinks of free Ca^{2+}; a situation that lends itself naturally to computational analysis. The approach for the majority of models to date has been to treat the cell as discrete compartments (representing the cytoplasm and intracellular organelles) that act as well-mixed reactors, isolated from a limitless extracellular space. Fluxes of Ca^{2+} occur between these compartments under the control of the various channels, transporters and buffers of the Ca^{2+} toolkit, combined with a finite leak across the membranes delimiting the compartments. Within this context, early attempts to simulate Ca^{2+} dynamics used simple empirical equations to describe the elements of the toolkit. The steady-state assumption was adopted, so that the activity of channels and pumps simply tracked IP_3 and Ca^{2+} concentration. Similarly, leak currents and buffering capacity were assumed to be linear or constant.

One of the earliest attempts to model Ca^{2+} oscillations in this way came from Meyer and Stryer [96]. These authors recognised that two of the key features of the system would be cooperative activation of Ca^{2+} release by IP_3, and positive feedback of Ca^{2+} at some stage in the pathway. The authors hypothesised that this positive feedback would arise from Ca^{2+} activating PLC, leading to enhanced IP_3 production. The model successfully generated Ca^{2+} oscillations, but also predicted that IP_3 concentration would oscillate in addition to Ca^{2+}. This behaviour was shown to be unnecessary in several experimental systems [5], and the model lost favour. A more persistently influential model was that of Goldbeter, Dupont and Berridge [51], which is based on the existence of two intracellular Ca^{2+} pools, one of which is sensitive to IP_3 and the other not. Consequently, receptor activation leads to release of Ca^{2+} from the IP_3-sensitive pool, which triggers Ca^{2+} induced Ca^{2+} release from the IP_3-insensitive pool (supplying positive feedback). With associated pump and leak currents, this minimal model successfully generated Ca^{2+} oscillations with features similar to those observed experimentally, arising from cycles of the pool emptying into, and refilling from, the cytosol. The Goldbeter–Dupont–Berridge model therefore incorporated two variables, the Ca^{2+} concentrations in the cytosol (Z) and the IP_3-insensitive pool (Y), which varied with time:

$$\dot{Z} = \nu_0 + \nu_1\beta - \nu_2 + \nu_3 + k_f Y - kZ\,, \tag{1a}$$

$$\dot{Y} = \nu_2 - \nu_3 - k_f V\,. \tag{1b}$$

The dot indicates a derivative with respect to time, i.e. $\dot{Z} = \mathrm{d}Z/\mathrm{d}t$. Here ν_0 is leak across plasma membrane, ν_1 is efflux from IP_3-sensitive stores (multiplied by the scaling constant β, which increases with PLC activation), ν_2 is uptake into the IP_3 -insensitive store, ν_3 is efflux from the IP_3-sensitive store, k_f is leak from the IP_3 -insensitive store, and k is efflux across the plasma membrane. The channels and pumps of the IP_3-insensitive store were described by empirical equations of the Hill form, such that:

$$\nu_2 = V_{M_2}\frac{Z^n}{K_2^n + Z^n}\,, \qquad \nu_3 = V_{M_3}\frac{Y^m}{K_R^m + Y^m}\frac{Z^p}{K_A^p + Z^p}\,, \tag{2}$$

where V_{M_i} are maximal rates of Ca^{2+} transport, K_R and K_A are threshold constants, and the coefficients n, m and p determine the cooperativity of the transporter/channel. A later refinement of this model [37] reduced the system to a single Ca^{2+} pool, as experimental results did not support the segregation of pools in many cell types.

These simple models were very successful in reproducing much of the non-linear behaviour of IP_3-induced Ca^{2+} signalling, which demonstrated that the complexity of cellular signalling could arise from simple principles of cooperativity and feedback regulation. Nevertheless, discrepancies with experimental evidence remained, in particular, the requirement for stores to empty during an oscillatory cycle [18]. This approach remains in common use, but as experimental data accumulated on the biophysical properties of the components of the toolkit, more detailed models incorporating this extra complexity, were introduced.

3 Mechanistic models

In the early 1990s, several groups [65, 105, 13, 45] published experimental evidence that the IP_3 receptor is regulated by Ca^{2+} in a biphasic manner: low concentrations of Ca^{2+} rapidly activate the receptor, whilst high concentrations inactivate the receptor more slowly. The functional consequence of this activity is positive feedback of Ca^{2+} release following the initial IP_3 signal, followed by negative feedback after cytosolic Ca^{2+} concentration has reached hundreds of nanomolar. This behaviour is sufficient to generate Ca^{2+} oscillations, and so the IP_3 receptor became a focus in efforts to model cellular Ca^{2+} dynamics. It also prompted a switch in approach from the use of empirical models that described the steady-state behaviour of the receptor, to the adoption of mechanistically realistic models that postulate the existence of multiple states of the receptor, with transitions between states determined by microscopic rate constants. Such an approach has distinct advantages; principally that these models can describe both the mass action kinetics of an ensemble of receptors, and the stochastic behaviour of individual molecules. Such a strategy has been highly successful in elucidating the relationships between structure and function in plasma membrane ion channels [26].

In the following sub-sections, we summarise a number of mechanistic models that have been proposed for key elements of the Ca^{2+} signalling toolkit.

3.1 The IP_3 receptor

An early and influential model was that of De Young and Keizer [34]. We will take this as our archetype for consideration of IP_3R models to date, and adopt its nomenclature for later models, wherever possible.

De Young and Keizer argue that a receptor consists of three binding sites: an activating and an inhibitory Ca^{2+} binding site as well as an activating IP_3 binding site. Therefore, the state of a receptor can be specified by a binary triplet $ijk \in [0,1]^3$. The first index represents the IP_3 binding site, the second the Ca^{2+} activating binding site, and the last the Ca^{2+} inhibiting binding site. An index equals 1 when a site is occupied and 0 otherwise. Hence the state 110 refers to IP_3 and Ca^{2+} bound to the activating sites, respectively, and an empty inhibiting Ca^{2+} binding site. The resulting eight states are shown in Fig. 1. The binding rate constants for IP_3 activation are given by a_1 and a_3, whereas a_2 and a_4 refer to Ca^{2+} inhibition. Ca^{2+} activation is controlled by a_5. The dissociation rates for the above processes are denoted by b_1 through b_5.

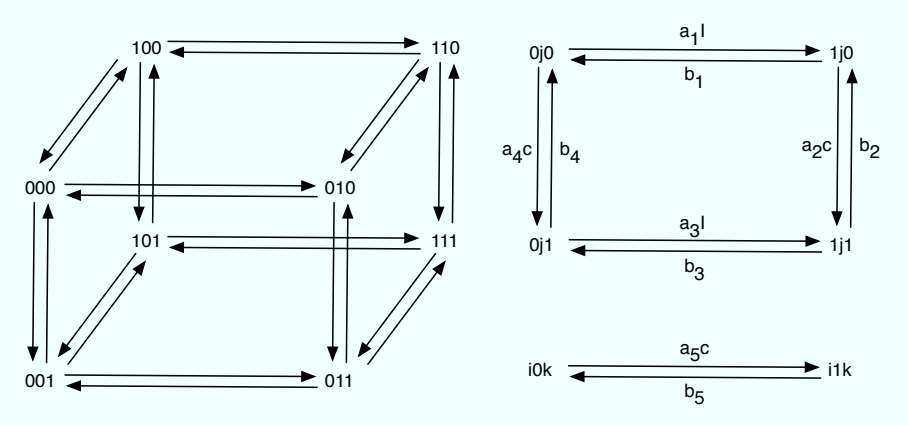

Fig. 1. Transition scheme of the De Young–Keizer model. See Table 1 for parameter values.

The reactions that occur at a receptor are binding and unbinding of Ca^{2+} and IP_3. They determine the state of one receptor. In an ensemble of receptors these processes lead to a fraction p_{ijk} of receptors in a state ijk. If the ensemble is large enough and homogeneous, these fractions can be described by rate equations. For instance, the time evolution of p_{110} is governed by

$$\dot{p}_{110} = -\left[b_5 + a_2 c + b_1\right] p_{110} + a_5 c p_{100} + b_2 p_{111} + a_1 I p_{010}\,, \tag{3}$$

with I being the IP_3 concentration and c the cytosolic Ca^{2+} concentration. The negative term on the right hand side represents the processes that reduce the value of p_{110}. This can result from unbinding of IP_3 with rate b_1, unbinding from the activating Ca^{2+} site with rate b_5 and binding to the inhibiting Ca^{2+} binding site with rate $a_2 c$. The remaining three terms control the increase of p_{110}. This happens for example through binding with rate $a_5 c$ to the activating Ca^{2+} site of a receptor that is in the state 100. Together with the remaining seven rate equations the state of the ensemble is fully characterised. We may discard one of these equations and use instead the conservation law

$a_1 = 400\ (\mu\text{Ms})^{-1}$	$d_1 = 0.13\ \mu\text{M}$
$a_2 = 0.2\ (\mu\text{Ms})^{-1}$	$d_2 = 1.049\ \mu\text{M}$
$a_3 = 400\ (\mu\text{Ms})^{-1}$	$d_3 = 943.3\ nM$
$a_4 = 0.2\ (\mu\text{Ms})^{-1}$	$d_4 = 144.5\ nM$
$a_5 = 20\ (\mu\text{Ms})^{-1}$	$d_5 = 82.34\ nM$

Table 1. Binding rate constants a_i and dissociation constants d_i, $i = 1, \ldots, 5$ of the De Young–Keizer model [34].

$$\sum_{\{ijk\}\in[0,1]^3} p_{ijk} = 1\,. \tag{4}$$

This states that each receptor belongs to one of the fractions p_{ijk} and that the number of receptors is conserved. In general the Ca^{2+} concentration is not constant in time, so that a closed solution for the fractions p_{ijk} is not accessible. However, we can compute the stationary values, $\bar{p}_{ijk}$, analytically. They read

$$\bar{p}_{000} = d_1 d_2 d_5 \gamma_1\,, \qquad \bar{p}_{100} = d_2 d_5 I \gamma_1\,, \tag{5a}$$

$$\bar{p}_{010} = d_1 d_2 \bar{c} \gamma_1\,, \qquad \bar{p}_{001} = d_3 d_5 \bar{c} \gamma_1\,, \tag{5b}$$

$$\bar{p}_{011} = d_3 \bar{c}^2 \gamma_1\,, \qquad \bar{p}_{101} = d_5 \bar{c} I \gamma_1\,, \tag{5c}$$

$$\bar{p}_{110} = d_2 \bar{c} I \gamma_1\,, \qquad \bar{p}_{111} = \bar{c}^2 I \gamma_1\,, \tag{5d}$$

with $\gamma_1^{-1} = (\bar{c} + d_5)(d_1 d_2 + \bar{c} d_3 + \bar{c} I + d_2 I)$. Here $d_i = b_i/a_i$ denotes the dissociation constants for IP_3 activation, Ca^{2+} activation and inhibition, respectively.

Table 1 shows the binding rate constants a_i and the dissociation constants d_i that De Young and Keizer used in their original work. Note that only 4 of the 5 dissociation constants are independent due to the thermodynamic constraint of detailed balance, i.e. $d_1 d_2 = d_3 d_4$ [60]. The constants in Table 1 were obtained by fitting steady state data by Bezprozvanny *et al.* [13]. This has lead to some criticism during the last years, because an IP_3 receptor almost never reaches a steady state under physiological conditions. The kinetic response to a change in the Ca^{2+} and IP_3 concentration seems to be more relevant for its role in intracellular Ca^{2+} dynamics. This idea was taken up by Sneyd *et al.* [132], suggesting a new set of parameter values based on superfusion experiments [36].

The IP_3 receptor is an integral part of the IP_3 receptor channel, through which Ca^{2+} is released from the endoplasmic reticulum. Biochemical experiments and electron microscopy revealed that the IP_3 receptor channel consists of 4 subunits and that it is conducting when at least 3 of the 4 subunits are activated [13, 156, 68]. In the De Young–Keizer model, the configuration with IP_3 and Ca^{2+} bound to the activating binding sites, but with an unoccupied Ca^{2+} inhibiting binding site is the activated state of the receptor. Consequently, the open probability of an IP_3 receptor channel is given by

$$p_o = 4p_{110}^3 - 3p_{110}^4\,. \tag{6}$$

Figure 2 depicts the stationary value of the open probability as a function of the Ca^{2+} concentration using equation (5). At low Ca^{2+} concentrations, an increase in Ca^{2+} leads to a significant increase in the open probability. However, when the Ca^{2+} concentration becomes too high, a further increase reduces the open probability. Such a bell shaped dependence of the stationary open probability on Ca^{2+} is present in a wide range of Ca^{2+} models (see e.g. section 3.2).

An alternative and simpler model to De Young–Keizer was proposed by Othmer and Tang [142], in which the binding of IP_3 and Ca^{2+} to the channels occurred sequentially (Fig. 3). This model consists of three coupled ordinary differential equations

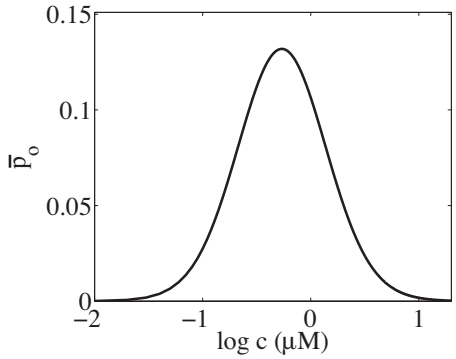

Fig. 2. Stationary value of the open probability $\overline{p}_o$ of an IP_3 receptor channel. Parameter values as in Table 1 and $I = 0.4$ μM.

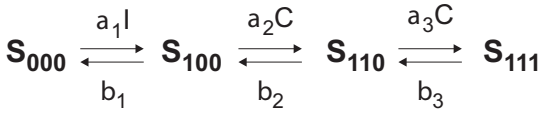

Fig. 3. Transition scheme of the Othmer–Tang model. See Table 2 for parameter values.

(ODEs), and was justified on the basis that experimental evidence suggested much faster binding of IP_3 and activating Ca^{2+} to the receptor than inactivating Ca^{2+} [142].

$a_1 = 12$ $(\mu\text{Ms})^{-1}$	$b_1 = 8$ s^{-1}
$a_2 = 15$ $(\mu\text{Ms})^{-1}$	$b_2 = 1.65$ s^{-1}
$a_3 = 0.8$ $(\mu\text{Ms})^{-1}$	$b_3 = 0.21$ s^{-1}

Table 2. Binding rate constants a_i and unbinding rates b_i, $i = 1, 2, 3$ of the Othmer–Tang model.

Bezprozvanny [12] introduced a further step to a simple sequential model of this type: a conformational change that was essential to the activation process (Fig. 4). This additional step allows the efficacy of channel opening, and thereby the open

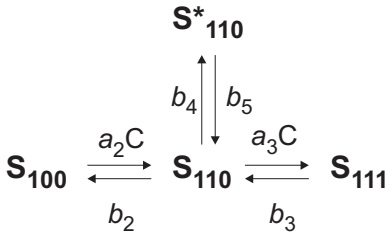

Fig. 4. Transition scheme of the Bezprozvanny model when IP_3 is already bound. See Table 3 for parameter values.

probability, to be fixed at a defined maximum, whereas earlier models could in principle yield higher open probabilities than are observed experimentally [13].

$a_3 = 4\ (\mu\text{Ms})^{-1}$	$b_3 = 0.8\ \text{s}^{-1}$
$b_4 = 25.2\ (\mu\text{Ms})^{-1}$	$b_5 = 224\ \text{s}^{-1}$

Table 3. Binding rate constant a_3, unbinding rate b_3, and transition rates b_4 and b_5 of the Bezprozvanny model when IP_3 is bound. The transition rate constant a_2 remains as an open parameter, but it fixes the unbinding rate $b_2 = 0.2\mu\text{M}\ a_2$.

Despite the advantages of a mechanistic approach, the system of ODEs that describes models of this type cannot be solved analytically, and so computationally-expensive numerical integrations must be carried out for non-equilibrium conditions. Accordingly, several attempts have been made to simplify the above models, based on the assumption of a quasi-steady state for those steps that are significantly faster than the rate limiting step.

The most commonly used simplification was introduced by Li and Rinzel [79]. They took advantage of the experimental findings that IP_3 and Ca^{2+} activation are much faster than Ca^{2+} inhibition. Consequently, they eliminated these two dynamics adiabatically, which resulted in a single equation for the fraction p_h of receptors that are not inactivated yet:

$$\dot{p}_h = -a_6 c p_h + b_6\,(1 - p_h)\ . \tag{7}$$

Here, the constants a_6 and b_6 are related to the parameters of the original De Young–Keizer model through $a_6 = a_2$ and $b_6 = b_2(I + d_1)/(I + d_3)$. With its single equation for an effective gating variable, the Li–Rinzel model represents the strongest approximation of the De Young–Keizer model. In some circumstances as e.g. the initiation stage of Ca^{2+} puffs, this might be too far a step, so that models with fewer eliminations were proposed, such as a 4-state model [41] or a 3-state model [149].

A comprehensive reduction of this type has been presented by Tang, Stephenson and Othmer [142]. These authors analysed the models discussed above and concluded that they can all be simplified to a single equation of a form that resembles that of a gating variable in the Hodgkin–Huxley formulation of action potential generation [142]:

$$\dot{y} = (y_\infty - y)/\tau\,, \tag{8}$$

where y is the fraction of receptors with Ca^{2+} bound to the inhibitory site. This simplification holds within certain ranges of parameters that result in quasi-steady states for binding interactions and conformational changes which are faster than receptor inactivation by Ca^{2+} binding. Strikingly, this simplified system can successfully model a range of the complex Ca^{2+} dynamics observed in cells [142].

Valuable as this approach has been in elucidating the core behaviours underlying non-equilibrium behaviour in Ca^{2+} signalling, it fails to accommodate some of the functional properties of IP_3 receptors in an experimental setting. Two new models that have extended mechanistic models in light of non-equilibrium experimental data obtained by rapid perfusion techniques [36, 90] have been recently published [128, 31].

Sneyd and Dufour [128] have elaborated on the traditional mass action deterministic model by incorporating a rapidly equilibriating step at each transition of the receptor between states. By making the equilibration dependent on Ca^{2+} concentration, the result is a model system in which transitions exhibit Ca^{2+} dependency, but with saturable rather than simple mass action kinetics. They illustrate this principle with the Ca^{2+}-dependent transition of receptor from an active (A) to inactive

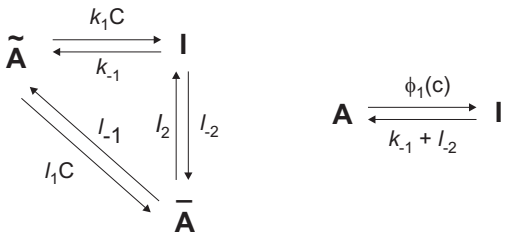

Fig. 5. Transition scheme of the Sneyd–Dufour model.

(I) state, as shown in Fig. 5. Here, the intermediates $\widetilde{\mathrm{A}}$ and $\bar{\mathrm{A}}$ are in instantaneous equilibrium, such that $c\widetilde{\mathrm{A}} = l_{-1}/l_1\bar{\mathrm{A}}$, where $c = [\mathrm{Ca}^{2+}]$. Therefore, as $\mathrm{A} = \widetilde{\mathrm{A}} + \bar{\mathrm{A}}$ the variation in the proportion of active receptors with time is described by:

$$p_A = (k_{-1} + l_{-2})\, p_I - \phi(c) p_A \,, \tag{9}$$

with

$$\phi(c) = \frac{c\,(k_1 l_{-1}/l_1 + l_2)}{c + l_{-1}/l_1} \,. \tag{10}$$

In effect, by postulating the existence of rapidly interconverting intermediates at each step of receptor activation/inactivation, the resultant model has a function of Ca^{2+} ($\phi(c)$) in place of the mass action constant of proportionality (k). This modification was introduced to accommodate the observation that the rate of receptor inactivation does not vary linearly with Ca^{2+} concentration (as would be predicted for a simple binding interaction), but its mechanistic basis is unclear.

A closer inspection of the scheme in Fig. 5 reveals that upon cycling through the states $\widetilde{\mathrm{A}}$, $\bar{\mathrm{A}}$, I and back to $\widetilde{\mathrm{A}}$, a Ca^{2+} ion is picked up in the first transition and is not released before the return to $\widetilde{\mathrm{A}}$. This can be overcome be introducing an additional state $\widetilde{\mathrm{I}}$ as proposed by Falcke [42] and recently implemented by Ullah and Jung [155].

Finally, Dawson, Lea and Irvine have introduced an "adaptive" model for the $\mathrm{IP_3R}$ [31], developed from a similar model for the ryanodine receptor [117]. The model postulates that the $\mathrm{IP_3R}$ exists in two gross conformational states (R and R′), in equilibrium, and that the conducting states of the channel can be reached only from one conformation (R). $\mathrm{IP_3}$ binds to the R′ state with slower kinetics, but higher affinity than the R state, and consequently, addition of $\mathrm{IP_3}$ results in a transient opening of the channel before equilibration shifts the majority of receptors into the (closed) R′ state. This scheme is summarised in Fig. 6.

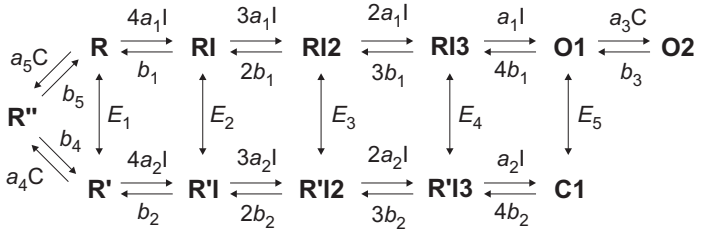

Fig. 6. Transition scheme of the Dawson–Lea–Irvine model. See Table 4 for parameter values.

In the simulations used by the authors in [31], the rate constant for $\mathrm{IP_3}$ binding to the R state (a_1) is ten times faster than the rate constant for binding to the R′ state

(a_2). Similarly, for the off rates, $b_1 = 100b_2$. The equilibrium constants for transition to the R′ state (shown here as E_i for simplicity) increasingly favour the R′ state as I increases (i.e. as more IP_3 molecules bind): $E_1 = e_1/e_{-1} = p_{R'}(\infty)/p_R(\infty) = 0.01$, whereas $E_5 = 100$. Therefore, if the rate at which equilibrium is reached is slower than the rate of binding to the R states, a step change in IP_3 concentration will result in a transient increase in the fraction of receptors reaching the open states (O1 and O2), followed by a slower progression to favour the C1 state as time passes.

$a_1 = 1000\ (\mu\text{Ms})^{-1}$	$b_1 = 1000\ \text{s}^{-1}$	$e_1 = 1\ \text{s}^{-1}$	$e_{-1} = 100\ \text{s}^{-1}$
$a_2 = 100\ (\mu\text{Ms})^{-1}$	$b_2 = 10\ \text{s}^{-1}$	$e_2 = 1\ \text{s}^{-1}$	$e_{-2} = 10\ \text{s}^{-1}$
$a_3 = 100\ (\mu\text{Ms})^{-1}$	$b_3 = 10\ \text{s}^{-1}$	$e_3 = 1\ \text{s}^{-1}$	$e_{-3} = 1\ \text{s}^{-1}$
$a_4 = 10\ (\mu\text{Ms})^{-1}$	$b_4 = 0.01\ \text{s}^{-1}$	$e_4 = 10\ \text{s}^{-1}$	$e_{-4} = 1\ \text{s}^{-1}$
$a_5 = 1\ (\mu\text{Ms})^{-1}$	$b_5 = 0.1\ \text{s}^{-1}$	$e_5 = 10\ \text{s}^{-1}$	$e_{-5} = 0.1\ \text{s}^{-1}$

Table 4. Binding rate constants a_i, unbinding rates b_i and transition rates e_i and e_{-i}, $i = 1, \ldots, 5$ of the Dawson–Lea–Irvine model.

The principal virtue of this model is the elegant mechanism by which quantal Ca^{2+} release is achieved. The IP_3R in this scenario opens in response to changes in IP_3 concentration, rather than giving a steady-state conductance at fixed IP_3 concentrations. This feature can also offer an explanation as to why unitary Ca^{2+} events are transient, and do not lead to uncontrolled positive feedback and global Ca^{2+} elevation. The authors took the model further, however, by incorporating the effect of a local domain of Ca^{2+} in the vicinity of the channel pore, by adding a second open state (O2), with higher open probability, which is reached by binding Ca^{2+}. Feedback of Ca^{2+} concentration in this way resulted in several effects: an increase in the cooperativity of IP_3 activation, dependence on luminal Ca^{2+} concentration (due to the pore microdomain), and a left shift in the IP_3 concentration response as receptor density increased. They also incorporated a Ca^{2+}-bound inactivated state (R″). These additional features can rationalise a large body of experimental work on quantal Ca^{2+} release, the existence of stores with different apparent IP_3 sensitivities, and the tendency for elementary Ca^{2+} events to occur in "hotspots", simply by postulating variation in the density of adaptive IP_3Rs in different regions of the cell ER. A final, cautionary note, is that the fitting of an empirical (Hill) equation to ensemble IP_3 concentration-response curves does not, necessarily, give any information about the underlying biophysics of individual receptors, as Hill coefficients larger than one (and adaptive kinetics) can be obtained even with a single IP_3 binding site.

We have only presented here an overview of some of the more popular IP_3R models. In fact there are many others, see for instance [1, 131, 87, 3]. For a recent review of IP_3R models see [129].

3.2 The Ryanodine receptor

Here we discuss ryanodine receptor modelling that relates specifically to the geometry of cardiac myocytes. This receptor resembles in many aspects the IP_3 receptor presented in section 3.1. For instance it is known that it can be activated or inhibited by Ca^{2+} [40, 54]. However, the close proximity of ryanodine receptor channels in the SR membrane and L-type Ca^{2+} channels in the plasma membrane has led to slightly different modelling approaches. Instead of considering a single receptor, the receptor channel as a whole is mostly modelled [136]. Figure 7 shows such a

gating scheme, which was proposed by Tang and Othmer [141]. Note the structural similarities to the IP_3 receptor model in Fig. 1. The binary tuple in Fig. 7 represents Ca^{2+} binding sites, with the first digit referring to activation and the second to inhibition. An index equals 1 when Ca^{2+} is bound and 0 otherwise. Hence, 10 refers to the state with Ca^{2+} bound only to the activating binding site.

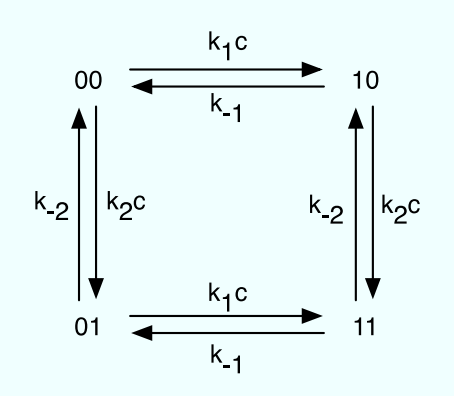

Fig. 7. Transition scheme of the Tang–Othmer model. See Table 5 for parameter values

In case of a large number of channels, the fraction of channels in a given state is determined by an equation similar to equation (3), e.g. we find for channels in the state 10

$$\dot{p}_{10} = -\left(k_2 c + k_{-1}\right) p_{10} + k_1 c p_{00} + k_{-2} p_{11} \,. \tag{11}$$

Since the Ca^{2+} concentration changes in time, solutions to equation (11) are not available in closed form. However, the stationary states can be readily computed, which yields

$$\overline{p}_{00} = K_1 K_2 \gamma_2 \,, \qquad \overline{p}_{10} = K_2 \bar{c} \gamma_2 \,, \tag{12a}$$

$$\overline{p}_{01} = K_1 \bar{c} \gamma_2 \,, \qquad \overline{p}_{11} = \bar{c}^2 \gamma_2 \,, \tag{12b}$$

with $\gamma_2^{-1} = K_1 K_2 + (K_1 + K_2)\bar{c} + \bar{c}^2$ and the dissociation constants $K_i = k_{-i}/k_i$. Note that $\overline{p}_{00} + \overline{p}_{01} + \overline{p}_{10} + \overline{p}_{11} = 1$ in analogy to equation (4). In a similar fashion to De Young and Keizer, Tang and Othmer consider the channel to be open when Ca^{2+} is only bound to the activating Ca^{2+} binding site, but not to the inhibiting. Hence, 10 represents the conducting state of the ryanodine receptor channel. Figure 8 depicts the stationary open probability $\overline{p}_{10}$ as a function of the Ca^{2+} concentration. We find a similar bell shaped curve as for the De Young–Keizer model.

The above analysis demonstrates that modelling IP_3 receptors and ryanodine receptors can proceed along the same lines, which greatly facilitates theoretical investigations of their dynamics. Yet, the prominent opposition of ryanodine receptor channels and L-type Ca^{2+} channels led early to the conclusion that geometry is crucial for the Ca^{2+} dynamics — an insight that is just about to make its breakthrough for IP_3 receptor channels.

When Ca^{2+} is liberated from the SR, it enters the tiny volume of the dyadic cleft, where it reaches concentrations as high as several hundred micromolar — orders of magnitude higher than bulk concentrations in a cell. Therefore, the gating mechanisms of the ryanodine receptor channel are not influenced by averaged concentrations, but by the highly elevated Ca^{2+} concentration in the dyadic cleft. Stern

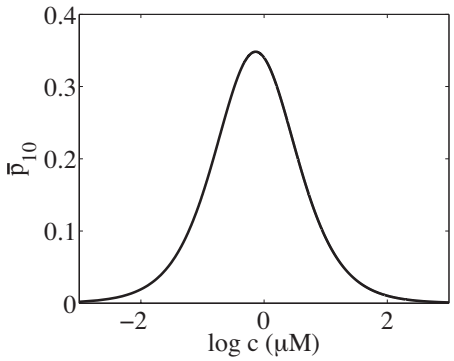

Fig. 8. Stationary value of the open probability $\bar{p}_{10}$ of the Tang–Othmer model.

took up this idea and proposed *local control* models [135]. They consist of separate equations that govern the time evolution of Ca^{2+} in the dyadic cleft, the rest of the cytosol, and the lumen, respectively. Since then, various aspects of the interplay between the geometry of the dyadic cleft and its dynamics have been discussed, see e.g. [108, 123, 143].

$k_1 = 15\ (\mu\text{Ms})^{-1}$	$k_{-1} = 7.6\ \text{s}^{-1}$
$k_2 = 0.8\ (\mu\text{Ms})^{-1}$	$k_{-2} = 0.84\ \text{s}^{-1}$

Table 5. Binding rate constants l_i and unbinding rates l_{-i}, $i = 1, 2$ of the Tang–Othmer model.

3.3 The SERCA pump

SERCA pumps belong to a group of enzymes known as P-type ATPases, so a natural step to model the dynamics of these pumps is to employ tools from enzyme kinetics [122]. The current picture as obtained by pharmacological studies and electromicroscopy [83, 153, 152] indicates that once cytosolic Ca^{2+} is bound to the ATPase, the enzyme undergoes several transformations including large conformational changes to the point when it releases Ca^{2+} into the lumen. A simplified model of this transport mechanism is depicted in Fig. 9. We assume that we can lump all intermediate states into two states: the state in which cytosolic Ca^{2+} is bound for the first time (IC_1), and the state from which Ca^{2+} is liberated into the lumen (IC_2). Consequently, the speed of the reaction is determined by the transitions between (IC_1) and (IC_2):

$$v = k_2\,[\text{IC}_1] - k_{-2}\,[\text{IC}_2]\ . \tag{13}$$

Using the steady-state approximation for binding of Ca^{2+} to the pump and for unbinding of Ca^{2+} from the pump, i.e. $[\text{IC}_1] = sc/K_1$ and $[\text{IC}_2] = se/K_2$ with $K_i = k_{-i}/k_i$ and e being the luminal Ca^{2+} concentration, we immediately arrive at

$$v = k_2\frac{sc}{K_1} - k_{-2}\frac{se}{K_2} = \frac{v_{m,f}sc/K_1 - v_{m,r}se/K_2}{s_T} = \frac{v_{m,f}c/K_1 - v_{m,r}e/K_2}{1 + c/K_1 + e/K_2}\,. \tag{14}$$

Here, $v_{m,f} = k_2 s_T$ and $v_{m,r} = k_{-2}s_T$ represent the maximal forward and reverse velocity, respectively, and $s_T = s + [\text{IC}_1] + [\text{IC}_2]$ denotes the total SERCA concentration because the pump can be either unbound (S) or in one of the internal

states IC_1 or IC_2. Note that since luminal Ca^{2+} can vary, the dynamics of e can have a strong impact on SERCA activity [158]. Equation (14) naturally incorporates that enzymatic reactions are reversible, and hence pays tribute to the experimental findings that SERCA pumps can operate in a reverse mode.

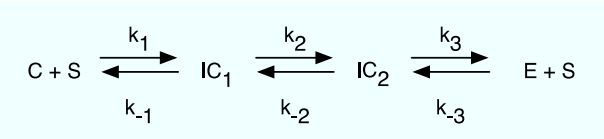

Fig. 9. Reaction scheme for a SERCA pump. The SERCA pump with no Ca^{2+} bound is denoted by S, whereas IC_1 and IC_2 refer to Ca^{2+} bound transition states. C and E refer to the cytosolic and luminal calcium.

The reaction scheme in Fig. 9 assumes that only one Ca^{2+} ion binds to the SERCA pump, which is then transported into the lumen. However, structural evidence has indicated that two ions are bound [152]. Assuming that they bind in a cooperative manner, equation (14) needs to be altered according to

$$v = \frac{v_{m,f}\,(c/K_1)^n - v_{m,r}\,(e/K_2)^n}{1 + (c/K_1)^n + (e/K_2)^n}\,, \tag{15}$$

where n represents the Hill index. Shannon *et al.* [123] give a value of $n = 1.6$.

The complexity of equation (15) often leads to the implementation of approximations. One frequently used assumption is that the luminal Ca^{2+} concentration is constant and does not feed back on the dynamics, so that Ca^{2+} is only pumped from the cytosol into the lumen. This leads to

$$v = v_{m,f}\,\frac{c^n}{K_1^n + c^n}\,. \tag{16}$$

The dominant feature of equations (15) and (16) is that the Ca^{2+} concentrations enter nonlinearly. In the limit of no cooperativity ($n = 1$) and low affinity ($c \ll K_1$ and $e \ll K_2$), both expressions can be linearised to yield

$$v = \frac{c}{\tau} - \frac{e}{\tau_e}\,, \tag{17}$$

or $v = c/\tau$, respectively, where we introduce the time scales $\tau = K_1/v_{m,f}$ and $\tau_e = K_2/v_{m,r}$. The advantage of the linearised expressions is that they allow us far reaching analytical investigations of intracellular Ca^{2+} dynamics, as we will illustrate later in section 5.

3.4 Mitochondria

Calcium transport by mitochondria involves mainly two pathways: uptake by a Ca^{2+} uniporter and release through a Na^+/Ca^{2+} exchanger (NCX). Like most of the cellular transport mechanisms, a convenient way of describing them is to resort to enzymatic reactions. The number of transporters remains unchanged in the course of a reaction in the same way as the total number of enzymes does not change. Following a review by Gunter and Pfeifer [53], the Na^+/Ca^{2+} exchanger is best represented by a product of 2 Hill functions:

$$v_{\mathrm{NCX}} = v_m^{\mathrm{NCX}} \frac{n^2}{K_n^2 + n^2} \frac{m}{K_m + m}\,, \tag{18}$$

where m and n denote the mitochondrial Ca^{2+} concentration and the cytosolic Na^+ concentration, respectively, and K_n and K_m refer to the dissociation constants for Na^+ and Ca^{2+} transport, respectively. The maximal velocity is given by v_m^{NCX}. Equation (18) reflects experimental findings that the Na^+/Ca^{2+} exchanger may work electrically neutral, in that it releases one Ca^{2+} ion for two Na^+ ions. However, other studies suggest a ratio larger than 2:1 (see e.g. [69]), which would lead to a higher Hill coefficient than 2 in equation (18). A similar controversy seems to exist for modelling the Ca^{2+} uniporter. Yet, the best fit is obtained for a Hill coefficient of 2 [53], giving rise to

$$v_{\mathrm{uni}} = v_m^{\mathrm{uni}} \frac{c^2}{K_u^2 + c^2}\,. \tag{19}$$

Here, v_m^{uni} is the maximal velocity of the uniporter, and K_u denotes the associated dissociation constant. Putting equations (18) and (19) together, the net Ca^{2+} flux of mitochondria is given by

$$J_m = v_{\mathrm{uni}} - v_{\mathrm{NCX}}\,. \tag{20}$$

Equation (20) represents a sensible starting point for incorporating mitochondrial dynamics into models of intracellular Ca^{2+}, because it captures essential experimental findings in a tractable expression. It has been successfully applied in [43, 44] to explain experiments in which energised mitochondria increase the speed of Ca^{2+} waves — a result that seems contradictory to the process of Ca^{2+} induced Ca^{2+} release (see section 4). We note that patch-clamp data from the inner mitochondrial membrane is available to guide further detailed modelling of the Ca^{2+} uniporter [77]. In case more details for the Ca^{2+} flux than equation (20) are needed such as coupling to the membrane potential of mitochondria or the concentration of ADP, see e.g. [86, 85, 84].

4 Homogenous cell models

A frequently used assumption in modelling cellular processes is that cells resemble well-stirred reactors, so that concentrations of any chemical compound are the same everywhere in the cell. Mathematically, this principle leads to a set of ODEs. When we focus just on the dynamics of cytosolic Ca^{2+} without fluxes over the plasma membrane, all these models possess the structure

$$\dot{c} = J_{\mathrm{release}}(X, c, t) + J_{\mathrm{leak}}(c, t) - J_{\mathrm{uptake}}(c, t)\,, \tag{21a}$$

$$\dot{X} = f(X, t)\,, \tag{21b}$$

where J_{release} and J_{leak} denote Ca^{2+} liberation through receptor channels and a leak current from internal Ca^{2+} stores, respectively, and J_{uptake} represents Ca^{2+} uptake from the cytosol into these stores. The variable X refers to the states of the receptors involved, and hence the release current explicitly depends on it.

We will illustrate the dynamics of equation (21) with the De Young–Keizer model introduced in section 3.1. As mentioned there, the open probability of an IP_3 receptor channel is given by equation (6), which reflects experimental findings that the channel is conducting when at least 3 of its 4 subunits are activated [13, 156, 68]. Consequently, we model the release current as

$$J_{\mathrm{release}} = k_c \left(4p_{110}^3 - 3p_{110}^4\right)(e - c)\,, \tag{22}$$

where k_c denotes its maximal value. The luminal Ca^{2+} concentration e is considered constant. Generally, a linear leak current $J_{\text{leak}} = -k_l c$ with a flux strength k_l is accepted, and the SERCA pumps are implemented by a Hill function as in equation (16) with a coefficient $n = 2$:

$$J_{\text{uptake}} = k_p \frac{c^2}{c^2 + K_p^2} \,. \tag{23}$$

Taking it together, the time evolution of the Ca^{2+} concentration as governed by equation (21) requires us to solve 8 coupled nonlinear ODEs.

An elegant insight into such high dimensional dynamics is obtained by computing bifurcation diagrams. The left panel of Fig. 10 depicts the stationary states of the Ca^{2+} concentration as a function of the IP_3 concentration. The prominent feature are two Hopf bifurcations [74]. If the IP_3 concentration is chosen in between these two bifurcation points, the Ca^{2+} concentration oscillates. A typical trace is shown in the right panel of Fig. 10. At low IP_3 concentrations, the Ca^{2+} dynamics possesses a linearly stable fixed point. The same is true for high IP_3 concentrations.

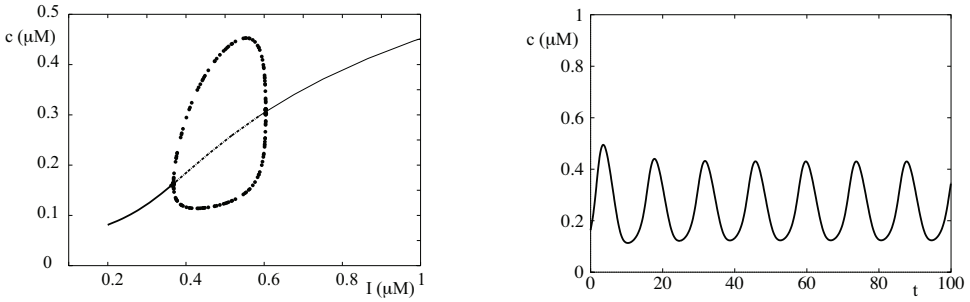

Fig. 10. Left: Bifurcation diagram of the De Young–Keizer model. Solid (dashed) lines represent stable (unstable) solutions. The minimum and the maximum of the oscillations are indicated by circles. Right: Typical Ca^{2+} oscillations for $I = 0.5$. μM. Parameter values as in table 1 and $k_c = 6\ \text{s}^{-1}$, $k_l = 0.108\ \text{s}^{-1}$, $k_p = 0.76\ (\mu\text{Ms})^{-1}$, $K_p = 0.1\ \mu$M, and $e = 1.69\ \mu$M.

The mechanism that underlies these oscillations is known as calcium induced calcium release (CICR). The open probability increases significantly with an increase of the Ca^{2+} concentration at low Ca^{2+} concentrations. Consequently, a gradual increase of Ca^{2+} at a closed IP_3 receptor channel might increase the open probability to such an extent that it opens. Then Ca^{2+} is liberated, and the high Ca^{2+} concentration inhibits the IP_3 receptor, leading to a closure of the channel. The Ca^{2+} concentration decreases and eventually reaches the same level as before the Ca^{2+} liberation started. Hence, the oscillation can start again. The features of an increase of the open probability at low Ca^{2+} concentrations and a decrease at high Ca^{2+} concentrations is also present in the stationary value of the open probability that is depicted in Fig. 2.

The occurrence of a Hopf bifurcation is one possibility to generate oscillations in spatially homogeneous Ca^{2+} models. Later approaches as e.g. in [1] found the same mechanism. However, it is not the only one. Another principle becomes apparent when we take X in equation (21) to be the Li–Rinzel model (equation (7)). The origin of the oscillations is best explained by investigating Fig. 11. It depicts the nullclines for c and p_h, i.e. the solutions to $\dot{c} = 0$ and $\dot{p}_h = 0$. The intersection of the two curves represents a linearly stable fixed point. When c and p_h take initial

values in the vicinity of the fixed point, they will always return to it. However, larger perturbations carry them away as indicated by the solid line. These excursions in phase space give rise to the observed oscillations and are known as *excitability* (see [81] for a comprehensive review). A more detailed analysis reveals that the present Ca^{2+} model possesses the same structure as the seminal equations by FitzHugh and Nagumo [46, 101]. Hence, the existence of excitability can be understood on general grounds.

Although Hopf bifurcations as well as excitability lead to oscillations, both mechanisms are fundamentally different. In the former case, oscillations exist intrinsically and persist forever if no perturbations are applied. On the contrast, oscillations in excitable systems can only be observed if the perturbations are strong enough. Therefore, noise can act in a destructive fashion in the presence of a Hopf bifurcation, but it is crucial in the regime of excitability. In the next section, we will explore the concept of excitability in more detail.

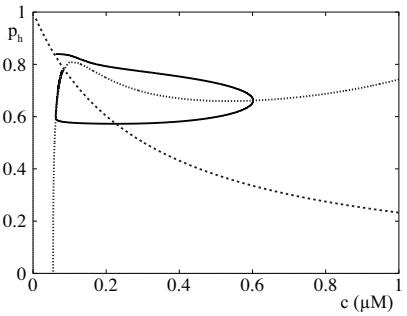

Fig. 11. Nullclines of c (dotted line) and p_h (dashed line) in the Li–Rinzel model. The solid line shows a trajectory with initial conditions $(c, p_h) = (0.06250, 0.83959)$. Parameter values as in Fig. 10 and $I = 0.2$ μM, $a_5 = 10$ $(\mu\text{Ms})^{-1}$.

5 Threshold models

We saw in section 4 that excitability is one mechanism to generate oscillations. Figure 12 illustrates that excitability is intimately related to threshold crossing. The notion of a perturbation being sufficiently strong is the same as indicating that a perturbation exceeds a threshold. If the initial perturbation is too weak, the Ca^{2+} concentration returns to its steady state. Otherwise, it crosses the threshold and evokes an oscillation.

In the case of the Li–Rinzel model, it is obvious that crossing the threshold and the exact form of the oscillation depends on both variables, the Ca^{2+} concentration c and the gating variable p_h. The latter summarises all the dynamics of the release channel, so that it essentially encodes for the state of the channel being either open or closed. Note that this discrete notion (on/off) is blurred by considering a population of channels and consequently fractions of open channels. This switch-like idea led to an approximation of equation (21) that is now known as a threshold model. Instead of considering the full gating mechanism as in equation (21b), this approach assumes that as long as the Ca^{2+} concentration is below a threshold, no release occurs, but as soon as it crosses threshold, Ca^{2+} is liberated from internal stores in a prescribed form. Consequently, equation (21) is replaced by a single equation with the new release term

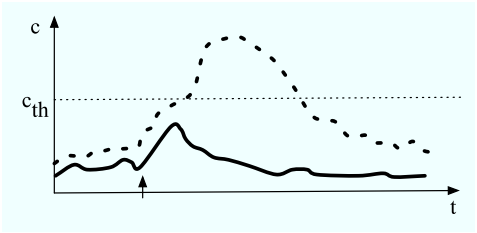

Fig. 12. Concept of excitability. At the time indicated by the arrow, both Ca^{2+} trajectories are perturbed. The solid line shows a subthreshold perturbation, whereas the dashed line represents a superthreshold perturbation.

$$J_{\text{release}} = \sum_i f(t - T_i)\,. \tag{24}$$

The release times T_i are defined by

$$T_i = \inf\left\{t \,|\, c \geq c_{\text{th}},\, t > T_{i-1} + \tau_R\right\}\,, \tag{25}$$

where τ_R denotes an absolute refractory time-scale. Equation (25) states that release occurs when the Ca^{2+} concentration is higher than a threshold value c_{th} and that there is at least a time τ_R between consecutive release events. Given a firing time T_i, the function $f(t)$ in equation (24) governs the exact shape of the Ca^{2+} release. Assuming that liberation lasts for a time Δ with a constant flux density η, it is common to write $f(t) = \eta\Theta(t - \Delta)\Theta(t)$, where Θ is the Heaviside function with $\Theta(t) = 1$ for $t \geq 0$ and 0 otherwise. One assumption in equation (24) is that Ca^{2+} release occurs at every point in the cell. However, it is well known that release sites form either regular lattices as in cardiac myocytes or a scattered randomly as in Xenopus oocytes [22, 88]. We can easily accommodate for such spatial arrangements by changing the release flux according to

$$J_{\text{release}} = \sum_{i,j} f(t - T_i^j)\delta(x_j - x)\,, \tag{26}$$

where $\delta(x)$ is a Dirac-delta function. Release occurs now at sites labelled by the index j, so that T_i^j is the ith release event at site j.

Threshold models have greatly facilitated studies of intracellular Ca^{2+} dynamics, since they allow far reaching analytical results and cheap numerical simulations [75, 107, 32, 27]. When using the form of release (26) such threshold models are called fire-diffuse-fire (FDF) models. Indeed they have contributed significantly to our understanding of Ca^{2+} fronts and spiral waves, which represent some of the most prominent Ca^{2+} patterns in cell biology. Note that to study wave phenomena in general, we need to append equation (21a) by a diffusive contribution, i.e.

$$\frac{\partial c}{\partial t} = D\frac{\partial^2}{\partial x^2}c + J_{\text{release}} + J_{\text{leak}}(c) - J_{\text{uptake}}(c)\,, \tag{27}$$

where D is the diffusion coefficient of cytosolic Ca^{2+}. For a general introduction to waves see [74, 100].

Using the release flux (26) the model is not translation invariant and one expects the emergence of saltatory waves, i.e. waves that do not propagate with a constant profile. Rather activity jumps from one release site to another, so that the speed of propagation is naturally defined in terms of the ratio of inter-release site distance to the duration of jumping. An example of such a wave is shown in Fig. 13.

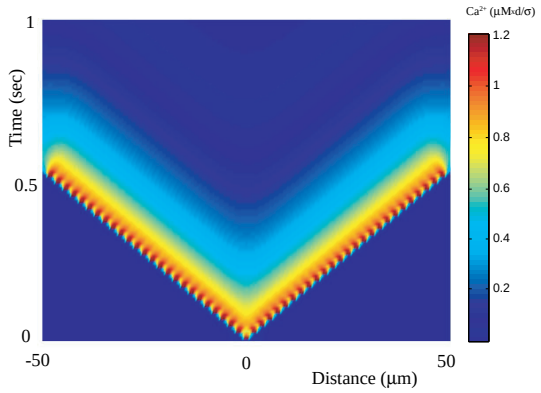

Fig. 13. An example of two saltatory pulses moving out from the center of a deterministic one dimensional FDF model with 50 regularly spaced release sites and free boundary conditions. Redrawn from [28].

Despite their successes, many threshold models assume that the luminal Ca^{2+} concentration remains constant. This is only true if the lumen is infinitely large and diffusion is very fast. How quickly Ca^{2+} diffuses in the lumen is still an open question, (see [103] and [76] for opposing views), but we can be sure about the finiteness of organelles. Consequently, a natural extension of equation (27) are the bidomain equations

$$\frac{\partial c}{\partial t} = D\frac{\partial^2 c}{\partial x^2} + J_{\text{release}}(c, c_{\text{er}}) + J_{\text{leak}}(c, c_{\text{er}}) - J_{\text{uptake}}(c, c_{\text{er}})\,, \tag{28a}$$

$$\frac{\partial c_{\text{er}}}{\partial t} = D_{\text{er}}\frac{\partial^2 c_{\text{er}}}{\partial x^2} - \frac{1}{\gamma}[J_{\text{release}}(c, c_{\text{er}}) + J_{\text{leak}}(c, c_{\text{er}}) - J_{\text{uptake}}(c, c_{\text{er}})]\,, \tag{28b}$$

$$J_{\text{release}}(c, c_{\text{er}}) = (c - c_{\text{er}}) \sum_{i,j} f(t - T_i^j)\delta(x_j - x)\,, \tag{28c}$$

where D_{er} and γ denote the diffusion coefficient of Ca^{2+} in the lumen and the ratio of luminal to cytosolic volume, respectively. This bidomain model has recently been employed to analyse a new dynamical phenomenon of back-and-forth rocking waves (for a model with a continuous distribution of stores: $T_i^j \to T_i(x)$) [151]. These types of waves have been observed in nemertean worm [137] and ascidian eggs [160]. They were first investigated in a biophysical model, with a Li–Rinzel model for the IP_3 receptor and a nonlinear SERCA pump (given by equations (7) and (16) respectively). Being reminiscent of a form of classical ballroom dance they were dubbed 'tango waves' [80]. Figure 14 shows different shapes of tango waves in a threshold bidomain model. The result in the left panel was obtained for a nonzero refractory time scale, and every time the main wave reverses direction, pulses are shed off. The number of pulses varies, as there is only one pulse for the first 4 reversals, but two pulses for the subsequent ones. The right panel illustrates that the back-and-forth movement can be more compact and that isolated pulses do not necessarily exist.

Although threshold models mimic deterministic excitable systems, they can be naturally extended to describe noisy systems. For instance, the value of the threshold may be chosen to fluctuate in such a way as to approximate the stochastic gating of receptors [61]. Stochastic calcium dynamics was investigated in [29, 28] and can give rise to noisy waves such as those seen in Fig. 15. The spark-to-wave transition in a particular stochastic threshold model is analysed in [73]. Interestingly, noise can

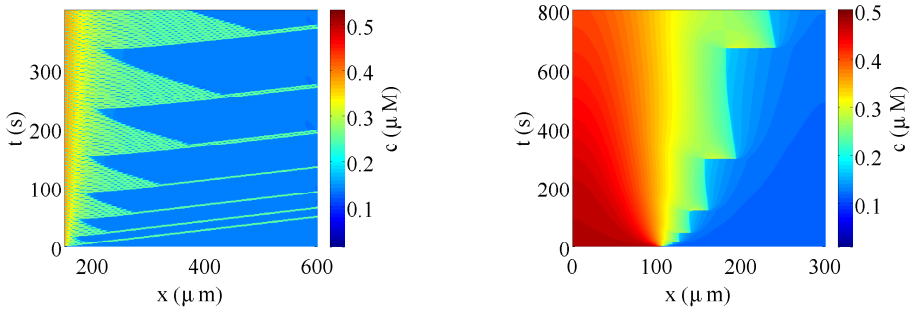

Fig. 14. Different kinds of tango waves in an FDF bidomain model with $\tau_R = 0.5$ s (left) and $\tau_R = 0$ s (right). The pseudocolour plot shows $c(x,t)$ in μM. For further details see [151].

have contrasting effects. On the one hand, it can lead to the extinction of waves that exist in the absence of noise. On the other hand, coherent oscillations can arise from a state of complete disorder, due to a form of array enhanced coherence resonance [28]. Indeed, noise can play a key role in shaping the dynamics of intracellular Ca^{2+}, and we will see some more examples of this in the next section.

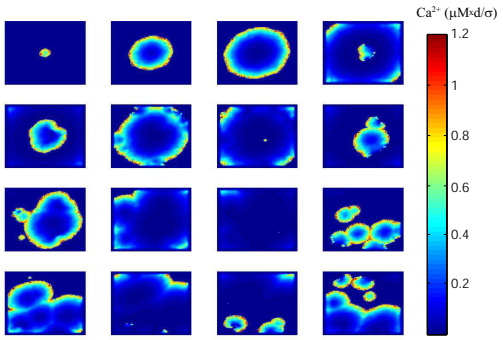

Fig. 15. Temporal sequence snapshots for a two-dimensional stochastic FDF model with low noise. Frames are presented every 0.45s starting in the top left corner and moving rightward and down. An initial seed in the center of the cell model leads to the formation and propagation of a circular front. Spiral waves form in the wake of the wave by spontaneous nucleation. These can be destroyed in wave–wave collisions and created by spontaneous nucleation. Redrawn from [28].

6 Stochastic modelling

Since the pioneering work of Hodgkin and Huxley [62], our understanding of ion channel dynamics has greatly improved, and today there is overwhelming experimental evidence that ion channels are intrinsically noisy. Although large populations of randomly gated ion channels can generate deterministic signals [47], detailed studies of intracellular Ca^{2+} dynamics reveal that fluctuations exist from the micro-scale of channels to the macro-scale of waves and oscillations [42].

The reason for this persistence lies in the spatial arrangement of the Ca^{2+} release channels. They are not homogeneously distributed in the cell, but they are grouped into clusters. Indeed, in the case of IP_3Rs there is some evidence that they prefer to occupy positions nearer to mitochondria [91]. The exact number of channels per clusters is still unknown, but estimates range between 5–100. More specifically, Swillens *et al.* reported cluster sizes between 5–40 for IP_3R channels [139]. More recent data for the number of IP_3Rs in a cluster can be found in [124]. These clusters can form either regular arrays as in the case of ryanodine receptor channels [48, 159, 64, 22], or they can be less ordered as in the case of IP_3R channels [88, 82].

This spatial organisation has far reaching effects. The small number of channels per cluster entails that the state of a cluster in terms of the states of the channels fluctuates strongly. Consequently, Ca^{2+} release through a cluster, which is determined by the number of open channels, does not generally show regular oscillations as in the right panel of Fig. 10. The interval between blips, puffs or sparks as well as the amplitude vary significantly [17, 138, 24, 89, 88]. From a modeller's perspective, this requires the replacement of the deterministic gating equations in section 3.1 by their stochastic counterparts.

The toolbox of stochastic processes offers different methods for this goal [49, 71, 111]. We will illustrate two of them with a stochastic version of the Li–Rinzel model (equation (7)), in which a receptor is either deactivated (D) or activated (A). Hence, it obeys the transition scheme

$$A \underset{b_6}{\overset{a_6 c}{\rightleftharpoons}} D\,. \tag{29}$$

The most fundamental approach is to write down a master equation for a channel with N receptors, which governs the time evolution of the probability $p_n(t)$ to find n receptors in the activated state at time t:

$$\frac{\mathrm{d}p_n(t)}{\mathrm{d}t} = -\left[na_6c + (N-n)b_6\right]p_n(t) + (n+1)a_6cp_{n+1}(t) + (N-n-1)\,b_6p_{n-1}(t)\,. \tag{30}$$

The negative term on the right hand side reflects that the probability decreases when any of the n activated receptors binds Ca^{2+} and hence deactivates, or when Ca^{2+} dissolves from any of the $(N-n)$ deactivated receptors. On the other hand, if there are $(n+1)$ activated receptors, binding of Ca^{2+} to one of them reduces this number to n activated receptors and hence increases the probability $p_n(t)$. Note that equation (30) is a system of N coupled equations, one for every n. Although being a basic equation, solving the master equation for more complicated gating schemes as e.g. the De Young–Keizer model is computationally expensive, so that approximations were suggested.

The two most frequently used approximations are either Fokker-Planck equations or Langevin equations. Instead of a set of N coupled equations, a Fokker-Planck equation is a single equation for the probability $p(x,t)$ to find a fraction $x = n/N$ receptors in the activated state. However, a master equation gives rise to several Fokker-Planck equations, which all have different properties. At the end the current question at hand decides upon a specific choice [50]. Following the ideas of Kramers and Moyal [78, 99], we find

$$\frac{\partial p(x,t)}{\partial t} = -\frac{\partial}{\partial x}\left[b_6(1-x) - a_6cx\right]p(x,t) + \frac{1}{2N}\frac{\partial^2}{\partial x^2}\left[b_6(1-x) + a_6cx\right]p(x,t)\,. \tag{31}$$

Both equations, (30) and (31), describe the time evolution of the *probability* to find some number or some fraction of activated subunits, respectively. Langevin took a different approach and wrote down an equation for the actually *value* of x:

$$\frac{\partial x}{\partial t} = [b_6(1-x) - a_6 c x]\, x + \sqrt{\frac{b_6(1-x) + a_6 c x}{N}}\xi(t)\,, \tag{32}$$

where $\xi(t)$ is zero-mean Gaussian white noise, i.e. the mean of ξ vanishes, $\langle \xi(t) \rangle = 0$, and the correlations obey $\langle \xi(t)\xi(t') \rangle = \delta(t - t')$ [119]. Note that equations (30) and (31) always give the same result for identical initial conditions, respectively, whereas equation (32) yields different outcomes for every run. This is due to the the Gaussian noise. It is worth noting that equation (31) and (32) are equivalent [49]. Which to choose depends on the specific question: if the probability distribution is needed, then the Fokker-Planck equation is the first choice, whereas the Langevin equation reveals how the fraction of activated channels actually evolves in time. Both approaches have been successfully used in the past to study various aspects of intracellular Ca^{2+} dynamics [126, 155, 70, 125, 95, 149].

That fluctuations at the cluster level are necessary for a functional Ca^{2+} dynamics becomes evident when we look at the Ca^{2+} concentrations that occur at a releasing cluster. Since liberation is spatially restricted, the Ca^{2+} concentration reaches values 2–3 orders of magnitude higher than bulk concentrations [146]. Note that the IP_3 receptors experience these highly elevated Ca^{2+} concentrations, and not the bulk concentration far away from the cluster. Without any noise, such a cluster would not be able to oscillate [147, 148]. The reason is that these high Ca^{2+} concentrations saturate any feedback mechanisms of the IP_3 receptor. However, they are the crucial element in driving oscillations, so that blocking them prevents the IP_3 receptors from oscillating.

We now move one structural level higher and consider a group of clusters. Taking up the idea of CICR mentioned in section 4, the distance of several microns between adjacent clusters entails that they are weakly coupled by the Ca^{2+} concentration, because only little Ca^{2+} diffuses from one open cluster to the next one. Consequently, the open probability of a still closed cluster increases only slightly by the opening of one of its neighbours. Release through a single cluster is therefore insufficient to trigger a Ca^{2+} wave, which travels through the cell. This was observed experimentally and in simulations, leading to the conclusion that a minimum number of adjacent clusters needs to liberate Ca^{2+} to start a wave [89, 2, 41]. The time that it takes to form such a critical nucleus of conducting clusters is truly random due to fluctuations on the single cluster level and the weak coupling between clusters. Therefore, the period of Ca^{2+} oscillations is a varying quantity that demonstrates the fluctuations of intracellular Ca^{2+} dynamics on the macroscopic scale.

The insight that fluctuations occur on vastly different time scales and length scales have rendered intracellular Ca^{2+} one of today's most challenging model systems. The goal of understanding cellular behaviour needs to start at the receptor level and has to take the real geometry of cells into account. First steps in integrating processes on the receptor level into higher order dynamics have been achieved, [28, 150], and it will be exciting to see how new modelling bridges between different cellular mechanisms will deepen our understanding of cellular responses.

7 Concluding remarks

The models described in this chapter constitute only a few examples of the efforts made to mathematically describe the complexities of the Ca^{2+} toolkit and how they impact on Ca^{2+} oscillations. It is clear that despite significant research into the biology that controls oscillations, not all parameters that govern the 'on' and

'off' mechanisms in Ca^{2+} signalling are known. Moreover, the isoform specific differences in the biophysics of the channels, pumps and exchangers as well as how they are affected by protein-protein interactions and secondary modifications such as phosphorylation are only just beginning to emerge. Further points to consider are the spatial and Ca^{2+} buffering properties of the compartment in which Ca^{2+} signalling occurs. In the context of Ca^{2+} oscillations, the compartment can be a dyadic cleft in skeletal muscle, a neuronal spine, the entire cytosol or even a group of connected cells. Despite these caveats, modelling has already helped to identify many of the key control processes in the generation, propagation and termination of Ca^{2+} oscillations. Through a continual dialogue between experimental data and mathematical simulations we can determine which simplifications are acceptable in a given cellular context, and make quantitative predictions about the behaviour of the system, which can be tested. Furthermore, where models fail to capture the essential features of an experimental system, unrecognised signalling interactions may be suggested and sought experimentally. Ultimately, it can be hoped that new insight will be gained into how cells encode and decode the Ca^{2+} signals that drive so many aspects of physiology.

References

[1] Atri A, Amundson J, Clapham D, Sneyd J (1993) A single pool model for intracellular calcium oscillations and waves in the Xenopus laevis oocyte. Biophysical Journal 65:1727–1739

[2] Bär M, Falcke M, Levine H, Tsimring LS (2000) Discrete stochastic modeling of calcium channel dynamics. Physical Review Letters 84:5664–5667

[3] Baran I (2005) Gating mechanisms of the type-1 inositol trisphosphate receptor. Biophysical Journal 89(2):979–998

[4] Bennett DL, Cheek TR, Berridge MJ, De Smedt H, Parys JB, Missiaen L, Bootman MD (1996) Expression and function of ryanodine receptors in nonexcitable cells. Journal of Biological Chemistry 271(11):6356–62

[5] Berridge MJ (1990) Calcium oscillations. Journal of Biological Chemistry 265(17):9583–9586

[6] Berridge MJ (1997) The AM and FM of calcium signalling. Nature 386(6627):759–60

[7] Berridge MJ, Galione A (1988) Cytosolic calcium oscillators. The FASEB Journal 2(15):3074–82

[8] Berridge MJ, Rapp PE (1979) A comparative survey of the function, mechanism and control of cellular oscillators. Journal of Experimental Biology 81:217–79

[9] Berridge MJ, Cobbold PH, Cuthbertson KS (1988) Spatial and temporal aspects of cell signalling. Philosophical Transactions of the Royal Society London B, Biological Sciences 320(1199):325–43

[10] Berridge MJ, Cheek TR, Bennett DL, Bootman MD (1995) Ryanodine receptors and intracellular calcium signalling. In: Sorrentino V (ed) Ryanodine receptors: A CRC Pharmacology & Toxicology Series, Basic and Clinical, CRC Press, pp 119–154

[11] Berridge MJ, Bootman MD, Roderick HL (2003) Calcium signalling: dynamics, homeostasis and remodelling. Nature Reviews Molecular Cell Biology 4(7):517–29

[12] Bezprozvanny I (1994) Theoretical analysis of calcium wave propagation based on inositol (1,4,5)-trisphosphate (InsP3) receptor functional properties. Cell Calcium 16(3):151–166

[13] Bezprozvanny I, Watras J, Ehrlich B (1991) Bell-shaped calcium-response curves of Ins(1,4,5)P_3- and calcium-gated channels from endoplasmic reticulum of cerebellum. Nature 351:751–754

[14] Bird GS, Rossier MF, Obie JF, Putney J J W (1993) Sinusoidal oscillations in intracellular calcium requiring negative feedback by protein kinase C. Journal of Biological Chemistry 268(12):8425–8

[15] Blatter LA, Wier WG (1992) Agonist-induced $[Ca^{2+}]_i$ waves and Ca^{2+}-induced Ca^{2+} release in mammalian vascular smooth muscle cells. American Journal of Physiology 263(2 Pt 2):H576–86

[16] Boitano S, Dirksen ER, Sanderson MJ (1992) Intercellular propagation of calcium waves mediated by inositol trisphosphate. Science 258(5080):292–5

[17] Bootman M, Niggli E, Berridge M, Lipp P (1997) Imaging the hierarchical Ca^{2+} signalling system in HeLa cells. The Journal of Physiology 499(Pt 2):307–314

[18] Bootman MD (1994) Quantal Ca^{2+} release from InsP3-sensitive intracellular Ca^{2+} stores. Molecular and Cellular Endocrinology 98(2):157–166

[19] Bootman MD, Berridge MJ (1996) Subcellular Ca^{2+} signals underlying waves and graded responses in HeLa cells. Current Biology 6(7):855–65

[20] Bootman MD, Young KW, Young JM, Moreton RB, Berridge MJ (1996) Extracellular calcium concentration controls the frequency of intracellular calcium spiking independently of inositol 1,4,5-trisphosphate production in HeLa cells. Biochemical Journal 314 (Pt 1):347–54

[21] Bootman MD, Berridge MJ, Roderick HL (2002) Calcium signalling: more messengers, more channels, more complexity. Current Biology 12(16):R563–5

[22] Bootman MD, Higazi DR, Coombes S, Roderick HL (2006) Calcium signalling during excitation-contraction coupling in mammalian atrial myocytes. Journal of Cell Science 119:3915–3925

[23] Bosanac I, Alattia JR, Mal TK, Chan J, Talarico S, Tong FK, Tong KI, Yoshikawa F, Furuichi T, Iwai M, Michikawa T, Mikoshiba K, Ikura M (2002) Structure of the inositol 1,4,5-trisphosphate receptor binding core in complex with its ligand. Nature 420(6916):696–700

[24] Callamaras N, Marchant JS, Sun XP, Parker I (1998) Activation and coordination of InsP3-mediated elementary Ca^{2+} events during global Ca^{2+} signals in Xenopus oocytes. The Journal of Physiology 509(1):81–91

[25] Carroll J, Swann K, Whittingham D, Whitaker M (1994) Spatiotemporal dynamics of intracellular $[Ca^{2+}]_i$ oscillations during the growth and meiotic maturation of mouse oocytes. Development 120(12):3507–17

[26] Colquhoun D, Hawkes AG (1995) The Principle of the Stochastic Interpretation of Ion-Channel Mechanics. In: Sakmann B, Neher E (eds) Single Channel Recording, Plenum Press, pp 397–482

[27] Coombes S (2001) The effect of ion pumps on the speed of travelling waves in the fire-diffuse-fire model of Ca^{2+} release. Bulletin of Mathematical Biology 63(1):1–20

[28] Coombes S, Timofeeva Y (2003) Sparks and waves in a stochastic fire-diffuse-fire model of Ca^{2+} release. Physical Review E 68:021,915–1–8

[29] Coombes S, Hinch R, Timofeeva Y (2004) Receptors, sparks and waves in a fire-diffuse-fire framework for calcium release. Progress in Biophysics and Molecular Biology 85:197–219

[30] Cuthbertson KS, Cobbold PH (1985) Phorbol ester and sperm activate mouse oocytes by inducing sustained oscillations in cell Ca^{2+}. Nature 316(6028):541–2

[31] Dawson AP, Lea EJ, Irvine RF (2003) Kinetic model of the inositol trisphosphate receptor that shows both steady-state and quantal patterns of Ca^{2+} release from intracellular stores. Biochemical Journal 370:621–629

[32] Dawson SP, Keizer J, Pearson JE (1999) Fire-diffuse-fire model of dynamics of intracellular calcium waves. Proceedings of the National Academy of Sciences USA 96(11):6060–6063
[33] De Koninck P, Schulman H (1998) Sensitivity of CaM kinase II to the frequency of Ca^{2+} oscillations. Science 279(5348):227–30
[34] De Young G, Keizer J (1992) A single inositol 1,4,5-triphosphate-receptor-based model for agonist-stimulated oscillations in Ca^{2+} concentration. Proc Natl Acad Sci USA 89:9895–9899
[35] Dolmetsch RE, Xu K, Lewis RS (1998) Calcium oscillations increase the efficiency and specificity of gene expression. Nature 392(6679):933–6
[36] Dufour JF, Arias IM, Turner TJ (1997) Inositol 1,4,5-trisphosphate and calcium regulate the calcium channel function of the hepatic inositol 1,4,5-trisphosphate receptor. Journal of Biological Chemistry 272(5):2675–2681
[37] Dupont G, Goldbeter A (1993) One-pool model for Ca^{2+} oscillations involving Ca^{2+} and inositol 1,4,5-trisphosphate as co-agonists for Ca^{2+} release. Cell Calcium 14(4):311–322
[38] Ehrlich BE (1995) Functional properties of intracellular calcium-release channels. Current Opinion in Neurobiology 5(3):304–9
[39] Espelt MV, Estevez AY, Yin X, Strange K (2005) Oscillatory Ca^{2+} signaling in the isolated Caenorhabditis elegans intestine: role of the inositol-1,4,5-trisphosphate receptor and phospholipases C beta and gamma. The Journal of General Physiology 126(4):379–92
[40] Fabiato A (1992) Two kinds of calcium-induced release of calcium from the sarcoplasmic reticulum of skinned cardiac cells. In: Frank GB, Bianchi CP, Keurs H (eds) Excitation-Contraction Coupling in Skeletal, Cardiac and Smooth Muscle, Advances in Experimental Medicine and Biology, vol 311, Springer, pp 245–262
[41] Falcke M (2003) On the role of stochastic channel behavior in intracellular Ca^{2+} dynamics. Biophysical Journal 84:42–56
[42] Falcke M (2004) Reading the pattern in living cells - the physics of Ca^{2+} signaling. Advances in Physics 53:255–440
[43] Falcke M, Hudson JL, Camacho P, Lechleiter JD (1999) Impact of mitochondrial Ca^{2+} cycling on pattern formation and stability. Biophysical Journal 77(1):37–44
[44] Falcke M, Li Y, Lechleiter JD, Camacho P (2003) Modeling the dependence of the period of intracellular Ca^{2+} waves on SERCA expression. Biophysical Journal 85(3):1474–1481
[45] Finch EA, Turner TJ, Goldin SM (1991) Calcium as a coagonist of inositol 1,4,5-trisphosphate-induced calcium release. Science 252(5004):443–6
[46] FitzHugh R (1961) Impulses and physiological states in theoretical models of nerve membrane. Biophysical Journal 1(6):445–466
[47] Fox RF, Lu Yn (1994) Emergent collective behavior in large numbers of globally coupled independently stochastic ion channels. Physical Review E 49(4):3421–3431
[48] Franzini-Armstrong C (1999) The sarcoplasmic reticulum and the control of muscle contraction. The FASEB Journal 13(9002):266S–270
[49] Gardiner C (2004) Handbook of Stochastic Methods, 3rd edn. Springer, Berlin
[50] Gitterman M, Weiss G (1991) Some comments on approximations to the master equation. Physica A 170:503–510
[51] Goldbetter A, Dupont G, Berridge M (1990) Minimal model for signal-induced Ca^{2+} oscillations and for their frequency encoding through protein phosphorylation. Proceedings of the National Academy of Sciences USA 87(4):1461–1465

[52] Gray PT (1988) Oscillations of free cytosolic calcium evoked by cholinergic and catecholaminergic agonists in rat parotid acinar cells. Journal of Physiology 406:35–53
[53] Gunter TE, Pfeiffer DR (1990) Mechanisms by which mitochondria transport calcium. American Journal of Physiology – Cell Physiology 258(5):C755–786
[54] Gyorke S, Fill M (1993) Ryanodine receptor adaptation: control mechanism of Ca^{2+}-induced Ca^{2+} release in heart. Science 260(5109):807–809
[55] Hajjar RJ, Bonventre JV (1991) Oscillations of intracellular calcium induced by vasopressin in individual fura-2-loaded mesangial cells. frequency dependence on basal calcium concentration, agonist concentration, and temperature. Journal of Biological Chemistry 266(32):21,589–94
[56] Hajnoczky G, Thomas AP (1997) Minimal requirements for calcium oscillations driven by the IP_3 receptor. The EMBO Journal 16(12):3533–43
[57] Hajnoczky G, Robb-Gaspers LD, Seitz MB, Thomas AP (1995) Decoding of cytosolic calcium oscillations in the mitochondria. Cell 82(3):415–24
[58] Halet G, Marangos P, Fitzharris G, Carroll J (2003) Ca^{2+} oscillations at fertilization in mammals. Biochemical Society Transactions 31(Pt 5):907–11
[59] Hamilton SL (2005) Ryanodine receptors. Cell Calcium 38(3-4):253–60
[60] Hill TL (1977) Free Energy Transduction in Biology. Academic Press
[61] Hille B (2001) Ion Channels of Excitable Membranes, 3rd edn. Sinauer Assoicates, Sunderland, MA USA
[62] Hodgkin AL, Huxley AF (1952) A quantitative description of membrane current and its application to conduction and excitation in nerve. Journal of Physiology 177(4):500–544
[63] Holl RW, Thorner MO, Mandell GL, Sullivan JA, Sinha YN, Leong DA (1988) Spontaneous oscillations of intracellular calcium and growth hormone secretion. Journal of Biological Chemistry 263(20):9682–5
[64] Hu XF, Liang X, Chen KY, Xie H, Xu Y, Zhu PH, Hu J (2005) Modulation of the oligomerization of isolated ryanodine receptors by their functional states. Biophysical Journal 89(3):1692–1699
[65] Iino M (1990) Biphasic Ca^{2+} dependence of inositol 1,4,5-trisphosphate-induced Ca release in smooth muscle cells of the guinea pig taenia caeci. The Journal of General Physiology 95(6):1103–1122
[66] Iino M, Endo M (1992) Calcium-dependent immediate feedback control of inositol 1,4,5-triphosphate-induced Ca^{2+} release. Nature 360(6399):76–8
[67] Jensen AM, Chiu SY (1990) Fluorescence measurement of changes in intracellular calcium induced by excitatory amino acids in cultured cortical astrocytes. Journal of Neuroscience 10(4):1165–75
[68] Jiang QX, Thrower EC, Chester DW, Ehrlich BE, Sigworth FJ (2002) Three-dimensional structure of the type 1 inositol 1,4,5-trisphosphate receptor at 24 å resolution. The EMBO Journal 21:3575–3581
[69] Jung DW, Baysal K, Brierley GP (1995) The Sodium-Calcium antiport of heart mitochondria is not electroneutral. Journal of Biological Chemistry 270(2):672–678
[70] Jung P, Shuai J (2001) Optimal sizes of ion channel clusters. Europhysics Letters 56(1):29–35
[71] van Kampen N (2001) Stochastic Processes in Physics and Chemistry. North-Holland, Amsterdam
[72] Kapur N, Mignery GA, Banach K (2007) Cell cycle-dependent calcium oscillations in mouse embryonic stem cells. American Journal of Physiology – Cell Physiology 292(4):C1510–8
[73] Keener J (2006) Stochastic calcium oscillations. IMA Journal of Mathematical Medicine and Biology 23:1–25
[74] Keener J, Sneyd J (1998) Mathematical Physiology. Springer, New York

[75] Keizer J, Smith GD, Ponce-Dawson S, Pearson JE (1998) Saltatory propagation of Ca^{2+} waves by Ca^{2+} sparks. Biophysical Journal 75(2):595–600
[76] Keller M, Kao JPY, Egger M, Niggli E (2007) Calcium waves driven by "sensitization" wave-fronts. Cardiovascular Research 74(1):39–45
[77] Kirichok Y, Krapivinsky G, Clapham DE (2004) The mitochondrial calcium uniporter is a highly selective ion channel. Nature 427:360
[78] Kramers H (1940) Brownian motion in a field of force and the diffusion model of chemical reactions. Physica 7:284–304
[79] Li Y, Rinzel J (1994) Equations for $InsP_3$ receptor-mediated $[Ca^{2+}]_i$ oscillations derived from a detailed kinetic model: A Hodgkin-Huxley like formalism. Journal of Theoretical Biology 166:461–473
[80] Li YX (2004) Tango waves in a bidomain model of fertilization calcium waves. Physica D 186:27–49
[81] Lindner B, García-Ojalvo J, Neiman A, Schimansky-Geier L (2004) Effects of noise in excitable systems. Physics Reports 392:321–424
[82] Machaca K (2004) Increased sensitivity and clustering of elementary Ca^{2+} release events during oocyte maturation. Developmental Biology 275(1):170–182
[83] MacLennan DH, Rice WJ, Green NM (1997) The mechanism of Ca^{2+} transport by sarco(endo)plasmic reticulum Ca^{2+}-ATPases. Journal of Biological Chemistry 272(46):28,815–28,818
[84] Magnus G, Keizer J (1997) Minimal model of beta-cell mitochondrial Ca^{2+} handling. American Journal of Physiology – Cell Physiology 273(2):C717–733
[85] Magnus G, Keizer J (1998) Model of beta-cell mitochondrial calcium handling and electrical activity. I. Cytoplasmic variables. American Journal of Physiology – Cell Physiology 274(4):C1158–1173
[86] Magnus G, Keizer J (1998) Model of beta-cell mitochondrial calcium handling and electrical activity. II. Mitochondrial variables. American Journal of Physiology – Cell Physiology 274(4):C1174–1184
[87] Mak DD, McBride SMJ, Foskett JK (2003) Spontaneous channel activity of the inositol 1,4,5-trisphosphate (InsP3) receptor (InsP3R). Application of allosteric modeling to calcium and InsP3 regulation of InsP3R single-channel gating. The Journal of General Physiology 122(5):583–603
[88] Marchant J, Parker I (2001) Role of elementary Ca^{2+} puffs in generating repetitive Ca^{2+} oscillations. The EMBO Journal 20:65–76
[89] Marchant J, Callamaras N, Parker I (1999) Initiation of IP_3-mediated Ca^{2+} waves in Xenopus oocytes. The EMBO Journal 18:5285–5299
[90] Marchant JS, Taylor CW (1998) Rapid activation and partial inactivation of inositol trisphosphate receptors by inositol trisphosphate. Biochemistry 37(33):11,524–11,533
[91] Marchant JS, Ramos V, Parker I (2002) Structural and functional relationships between Ca^{2+} puffs and mitochondria in *Xenopus* oocytes. American Journal of Physiology – Cell Physiology 282:C1374–1386
[92] Marks PW, Maxfield FR (1990) Transient increases in cytosolic free calcium appear to be required for the migration of adherent human neutrophils. Journal of Cell Biology 110(1):43–52
[93] Maruyama Y, Inooka G, Li YX, Miyashita Y, Kasai H (1993) Agonist-induced localized Ca^{2+} spikes directly triggering exocytotic secretion in exocrine pancreas. The EMBO Journal 12(8):3017–22
[94] McAinsh MR, Webb A, Taylor JE, Hetherington AM (1995) Stimulus-induced oscillations in guard cell cytosolic free calcium. Plant Cell 7(8):1207–1219
[95] Meinhold L, Schimansky-Geier L (2002) Analytic description of stochastic calcium-signaling periodicity. Physical Review E 66(5):050,901

[96] Meyer T, Stryer L (1988) Molecular model for receptor-stimulated calcium spiking. Proceedings of the National Academy of Sciences USA 85(14):5051–5055

[97] Missiaen L, Taylor CW, Berridge MJ (1991) Spontaneous calcium release from inositol trisphosphate-sensitive calcium stores. Nature 352(6332):241–4

[98] Miyazaki S, Ito M (2006) Calcium signals for egg activation in mammals. Journal of Pharmacological Sciences 100(5):545–52

[99] Moyal J (1949) Stochastic processes and statistical physics. Journal of the Royal Statistical Society: Series B 11:150–210

[100] Murray JD (2004) Mathematical Biology. Springer, Berlin

[101] Nagumo J, Arimoto S, Yoshizawa S (1962) An active pulse transmission line simulating nerve axon. Proceedings of the Institute of Radio Engineers 50(10):2061–2070

[102] Neylon CB, Irvine RF (1990) Synchronized repetitive spikes in cytoplasmic calcium in confluent monolayers of human umbilical vein endothelial cells. FEBS Letters 275(1-2):173–6

[103] Olveczky BP, Verkman AS (1998) Monte Carlo analysis of obstructed diffusion in three dimensions: Application to molecular diffusion in organelles. Biophysical Journal 74(5):2722–2730

[104] Orchard CH, Eisner DA, Allen DG (1983) Oscillations of intracellular Ca^{2+} in mammalian cardiac muscle. Nature 304(5928):735–8

[105] Parker I, Ivorra I (1990) Inhibition by Ca^{2+} of inositol trisphosphate-mediated Ca^{2+} liberation: A possible mechanism for oscillatory release of Ca^{2+}. Proceedings of the National Academy of Sciences USA 87(1):260–264

[106] Parker I, Ivorra I (1990) Localized all-or-none calcium liberation by inositol trisphosphate. Science 250(4983):977–9

[107] Pearson JE, Ponce-Dawson S (1998) Crisis on skid row. Physica A 257(1-4):141–148

[108] Peskoff A, Langer G (1998) Calcium concentration and movement in the ventricular cardiac cell during an excitation-contraction cycle. Biophysical Journal 74(1):153–174

[109] Petersen CC, Toescu EC, Petersen OH (1991) Different patterns of receptor-activated cytoplasmic Ca^{2+} oscillations in single pancreatic acinar cells: dependence on receptor type, agonist concentration and intracellular Ca^{2+} buffering. The EMBO Journal 10(3):527–33

[110] Prentki M, Glennon MC, Thomas AP, Morris RL, Matschinsky FM, Corkey BE (1988) Cell-specific patterns of oscillating free Ca^{2+} in carbamylcholine-stimulated insulinoma cells. Journal of Biological Chemistry 263(23):11,044–7

[111] Risken H (1984) The Fokker-Planck equation. Springer, Berlin

[112] Robb-Gaspers LD, Thomas AP (1995) Coordination of Ca^{2+} signaling by intercellular propagation of Ca^{2+} waves in the intact liver. Journal of Biological Chemistry 270(14):8102–7

[113] Roderick HL, Bootman MD (2003) Bi-directional signalling from the InsP3 receptor: regulation by calcium and accessory factors. Biochemical Society Transactions 31(Pt 5):950–3

[114] Roderick HL, Berridge MJ, Bootman MD (2003) Calcium-induced calcium release. Current Biology 13(R425)

[115] Rooney TA, Sass EJ, Thomas AP (1989) Characterization of cytosolic calcium oscillations induced by phenylephrine and vasopressin in single fura-2-loaded hepatocytes. Journal of Biological Chemistry 264(29):17,131–41

[116] Rooney TA, Sass EJ, Thomas AP (1990) Agonist-induced cytosolic calcium oscillations originate from a specific locus in single hepatocytes. Journal of Biological Chemistry 265(18):10,792–6

[117] Sachs F, Qin F, Palade P (1995) Models of Ca^{2+} release channel adaptation. Science 267:2010–2011

[118] Sage SO, Adams DJ, van Breemen C (1989) Synchronized oscillations in cytoplasmic free calcium concentration in confluent bradykinin-stimulated bovine pulmonary artery endothelial cell monolayers. Journal of Biological Chemistry 264(1):6–9

[119] Schimansky-Geier L, Talkner P (2003) Tools of Stochastic Dynamics. In: Ebeling W, Schimansky-Geier L, Romanovsky YM (eds) Stochastic Dynamics of Reacting Biomolecules, World Scientific

[120] Schlegel W, Winiger BP, Mollard P, Vacher P, Wuarin F, Zahnd GR, Wollheim CB, Dufy B (1987) Oscillations of cytosolic Ca^{2+} in pituitary cells due to action potentials. Nature 329(6141):719–21

[121] Schulman H, Hanson PI, Meyer T (1992) Decoding calcium signals by multifunctional CaM kinase. Cell Calcium 13(6-7):401–11

[122] Segel IH (1976) Biochemical Calculations. John Wiley

[123] Shannon TR, Wang F, Puglisi J, Weber C, Bers DM (2004) A mathematical treatment of integrated Ca dynamics within the ventricular myocyte. Biophysical Journal 87(5):3351–3371

[124] Shuai J, Rose HJ, Parker I (2006) The number and spatial distribution of IP_3 receptors underlying calcium puffs in *Xenopus* oocytes. Biophysical Journal 91(11):4033–4044, DOI 10.1529/biophysj.106.088880

[125] Shuai JW, Jung P (2002) Optimal intracellular calcium signalling. Physical Review Letters 88(6):068,102–1–4

[126] Shuai JW, Jung P (2002) Stochastic properties of Ca^{2+} release of inositol 1,4,5-trisphosphate receptor clusters. Biophysical Journal 83(1):87–97

[127] Smith PM, Gallacher DV (1992) Acetylcholine- and caffeine-evoked repetitive transient Ca^{2+}-activated K^+ and C1- currents in mouse submandibular cells. Journal of Physiology 449:109–20

[128] Sneyd J, Dufour JF (2002) A dynamic model of the type-2 inositol trisphosphate receptor. Proceedings of the National Academy of Sciences USA 99(4):2398–2403

[129] Sneyd J, Falcke M (2005) Models of the inositol trisphosphate receptor. Progress in Biophysics and Molecular Biology 89(3):207–245

[130] Sneyd J, Tsaneva-Atanasova K (2003) Modeling calcium waves. In: Falcke M, Malchow D (eds) Understanding Calcium Dynamics - Experiments and Theory, Lecture Notes in Physics, Springer, Berlin, pp 179–199

[131] Sneyd J, LeBeau A, Yule D (2000) Traveling waves of calcium in pancreatic acinar cells: model construction and bifurcation analysis. Physica D 145(1-2):158–179

[132] Sneyd J, Falcke M, Dufour JF, Fox C (2004) A comparison of three models of the inositol trisphosphate receptor. Progress in Biophysics and Molecular Biology 85(2-3):121–140

[133] Sorrentino V (2004) Molecular determinants of the structural and functional organization of the sarcoplasmic reticulum. Biochimica at Biophysica Acta 1742(1-3):113–8

[134] Sorrentino V, Volpe P (1993) Ryanodine receptors: how many, where and why? Trends in Pharmacological Sciences 14(3):98–103

[135] Stern MD (1992) Theory of excitation-contraction coupling in cardiac muscle. Biophysical Journal 63(2):497–517

[136] Stern MD, Song LS, Cheng H, Sham JSK, Yang HT, Boheler KR, Rios E (1999) Local control models of cardiac excitation-contraction coupling. A possible role for allosteric interactions between ryanodine receptors. The Journal of General Physiology 113(3):469–489

[137] Stricker SA (1996) Repetitive calcium waves induced by fertilization in the nemertean worm Cerebratulus lacteus. Developmental Biology 176(2):243–263
[138] Sun X, Callamaras N, Marchant J, Parker I (1998) A continuum of $InsP_3$-mediated elementary Ca^{2+} signalling events in Xenopus oocytes. The Journal of Physiology 509:67–80
[139] Swillens S, Dupont G, Combettes L, Champeil P (1999) From calcium blips to calcium puffs: Theoretical analysis of the requirements for interchannel communication. Proceedings of the National Academy of Sciences USA 96:13,750–13,755
[140] Tang RH, Han S, Zheng H, Cook CW, Choi CS, Woerner TE, Jackson RB, Pei ZM (2007) Coupling diurnal cytosolic Ca^{2+} oscillations to the CAS-IP3 pathway in Arabidopsis. Science 315(5817):1423–6
[141] Tang Y, Othmer HG (1994) A model of calcium dynamics in cardiac myocytes based on the kinetics of ryanodine-sensitive calcium channels. Biophysical Journal 67(6):2223–2235
[142] Tang Y, Stephenson JL, Othmer HG (1996) Simplification and analysis of models of calcium dynamics based on IP_3-sensitive calcium channel kinetics. Biophysical Journal 70(1):246–263
[143] Tanskanen AJ, Greenstein JL, Chen A, Sun SX, Winslow RL (2007) Protein geometry and placement in the cardiac dyad influence macroscopic properties of calcium-induced calcium release. Biophysical Journal 92(10):3379–3396
[144] Taylor CW, da Fonseca PC, Morris EP (2004) Ip(3) receptors: the search for structure. Trends in Biochemical Sciences 29(4):210–9
[145] Thomas AP, Bird GS, Hajnoczky G, Robb-Gaspers LD, Putney J J W (1996) Spatial and temporal aspects of cellular calcium signaling. The FASEB Journal 10(13):1505–17
[146] Thul R, Falcke M (2004) Release currents of IP_3 receptor channel clusters and concentration profiles. Biophysical Journal 86:2660–2673
[147] Thul R, Falcke M (2004) Stability of membrane bound reactions. Physical Review Letters 93:188,103–1–4
[148] Thul R, Falcke M (2005) Reactive clusters on a membrane. Physical Biology 2:51–59
[149] Thul R, Falcke M (2006) Frequency of elemental events of intracellular calcium. Physical Review E 73(6):061,923–14
[150] Thul R, Falcke M (2007) Waiting time distributions for clusters of complex molecules. Europhysics Letters 79:38,003
[151] Thul R, Smith GD, Coombes S (2007) A bidomain threshold model of intracellular calcium release and propagating calcium waves. Journal of Mathematical Biology in press
[152] Toyoshima C, Nomura H (2002) Structural changes in the calcium pump accompanying the dissociation of calcium. Nature 418(6898):605–611
[153] Toyoshima C, Nakasako M, Nomura H, Ogawa H (2000) Crystal structure of the calcium pump of sarcoplasmic reticulum at 2.6 å resolution. Nature 405(6787):647–655
[154] Ueda S, Oiki S, Okada Y (1986) Oscillations of cytoplasmic concentrations of Ca^{2+} and K^+ in fused L cells. Journal of Membrane Biology 91(1):65–72
[155] Ullah G, Jung P (2006) Modeling the statistics of elementary calcium release events. Biophysical Journal 90(10):3485–3495
[156] Watras J, Bezprozvanny I, Ehrlich B (1991) Inositol 1,4,5-trisphosphate-gated channels in cerebellum: presence of multiple conductance states. Journal of Neuroscience 11:3239–3245
[157] Yada T, Oiki S, Ueda S, Okada Y (1986) Synchronous oscillation of the cytoplasmic Ca^{2+} concentration and membrane potential in cultured epithelial cells (intestine 407). Biochimica et Biophysica Acta 887(1):105–12

[158] Yano K, Petersen O, Tepikin AV (2004) Dual sensitivity of sarcoplasmic/endoplasmic Ca^{2+}-ATPase to cytosolic and endoplasmic reticulum Ca^{2+} as a mechanism of modulating cytosolic Ca^{2+} oscillations. Biochemical Journal 15(383 (Pt 2)):353–360

[159] Yin CC, Lai FA (2000) Intrinsic lattice formation by the ryanodine receptor calcium-release channel. Nature Cell Biology 2(9):669–671

[160] Yoshida M, Sensui N, Inoue T, Morisawa M, Mikoshiba K (1998) Role of two series of Ca^{2+} oscillations in activation of ascidian eggs. Developmental Biology 203(1):122–133